EXPERIMENTAL INVESTIGATION OF FLOW CHARACTERISTICS OVER SEMI-CIRCULAR BROAD CRESTED WEIR MODELS

BY

UMAR ABDULLAHI B.ENG (A.B.U, 2008)
M.Sc./ENG/0994/2010-2011

DEPERTMENT OF WATER RESOURCES AND ENVIRONMENTAL ENGINEERING,
FACULTY OF ENGINEERING
AHMADU BELLO UNIVERSITY, ZARIA NIGERIA

SEPTEMBER 2014

EXPERIMENTAL INVESTIGATION OF FLOW CHARACTERISTICS OVER SEMI-CIRCULAR BROAD CRESTED WEIR MODELS

BY

UMAR ABDULLAHI B.ENG (A.B.U, 2008)
M.Sc./ENG/0994/2010-2011

A THESIS SUBMITTED TO THE SCHOOL OF POST GRADUATE STUDIES AHMADU BELLO UNIVERSITY, ZARIA IN PARTIAL FULFILMENT OF THE REQUIREMENTS FOR THE AWARD OF MASTERS OF SCIENCE IN WATER RESOURCES AND ENVIRONMENTAL ENGINEERING.

DEPARTMENT OF WATER RESOURCES AND ENVIRONMENTAL ENGINEERING, FACULTY OF ENGINEERING
AHMADU BELLO UNIVERSITY, ZARIA, NIGERIA

SEPTEMBER 2014

DECLARATION

I hereby declare that the work in this thesis titled "Experimental Investigation of Flow Characteristics over Semi-Circular Broad Crested Weir" was performed by me in the Department of Water Resources and Environmental Engineering, under the supervision of Dr. Ismail Abubakar and Dr. D.B. Adie. The information derived from the literature has been duly acknowledged in the text and a list of references provided. No part of this work has been presented for another degree or diploma at any institution.

---------- ----------

UMAR ABDULLAHI **DATE**

M.Sc/ENG/0994/2010-11

CERTIFICATION

This is to certify that this thesis "Experimental Investigation of Flow Characteristics over Semi-Circular Crested Weir Models" by UMAR, ABDULLAHI meets the regulations governing the award of the degree of M.Sc. (Water Resources and Environmental Engineering) Ahmadu Bello University, and is approved for its contribution to knowledge and literary presentation.

---------- ----------

Dr. A. Ismail
Chairman, Supervisory Committee **Date**

---------- ----------

Dr. D.B Adie
Member, Supervisory Committee **Date**

---------- ----------

Dr. D.B. Adie
Head of Department **Date**

---------- ----------

Prof. A.A. Joshua
Dean Postgraduate School **Date**

DEDICATION

This thesis is dedicated to Allah (S.W.A) who has given me the strength to shoulder this responsibility. To my parents Mallam Jibrin Umaru and Mallama Amina Umaru for the roles they have played in my humble life; and also, to my family, friends and colleagues who have encouraged me to be patient and hard working.

ACKNOWLEDGEMENT

My unending gratitude goes to my parents; Mallam Jibrin Umaru and Mallama Amina Umaru for their parental upbringing and both have been supportive of my study of engineering. May Almighty Allah reward, bless and forgive your sins, Amin.

I appreciate the thorough supervision and guidance provided by Engr. (Dr.) Abubakar Ismail and Engr. (Dr.) D.B Adie as my major and minor supervisors respectively. During the research work I learnt from their inspiring guidance and enthusiastic daily work. I wouldn't have overcome my mistakes and fault without their help. I am also grateful to Prof. C.A Okoufu and Engr. (Dr.) J. A Otun, both are lecturers in the Department for their contributions, encouragement and support during the study.

I thank all those who constitute my thesis committee, sharing their knowledge, experiences, guidance and judgments were privileges to me. My thanks also to the hydraulic laboratory staff; Mr. C. Salami, Mr. S. Kajang, Mr. A Luka for arranging the necessary facilities for conducting my research work.

Special thanks go to other lecturers of the Department of Water Resources and Environmental Engineering especially Engr. (Dr.) S.B. Igboro, Engr. (Dr.) M.A.Ajibike, Engr. (Dr.) Fatima Badru, Engr. S.B Saulawa, Engr. Salihu Lukman, Engr. A. Argungu, Engr. B.K. Adeogun, Engr. M. M. Mujahid, Engr. Sani Ismail, Engr. Aliyu Adamu, Mr. P.C. Alika, Mal. G. Bello, Mr. G. Ameh, Mal. Y. Yahaya and Mrs. Akinwande the departmental secretary for various suggestions, contributions and encouragements rendered. Especially, the devotion of Salihu Lukman, B. Saulawa and M.M Mujahid in sourcing for me materials (journals) which have greatly contributed in accomplishing this research.

My friends, M.Sc. colleagues and well wishers who contributed in one way or another in my educational career are too numerous to mention here. My final word is that 'may Allah reward you all abundantly'.

TABLE OF CONTENTS

Title page		**i**
Declaration		**ii**
Certification		**iii**
Dedication		**iv**
Acknowledgement		**v**
Table of Content		**vi**
List of Plates		**ix**
List of Figures		**x**
List of Tables		**xi**
Abbreviation and Symbols		**xiii**
Abstract		**xvii**
CHAPTER ONE: INTRODUCTION		**1**
1.1	Introduction	1
1.2	Aim and Objectives of the Study	3
1.3	Statement of Research Problem	4
1.4	Justification	4
1.5	Scope of Study	4
CHAPTER TWO: LITERATURE REVIEW		**5**
2.1	Theoretical Consideration	5
2.2	Discharge Equation	6
2.3	Dimensional Analysis of a Sharp Crested Weir	8
2.4	Weir Equation	9
2.5	Previous Studies on Weir Equations	9

2.6 Previous Studies on Oblique Weirs 11

2.7 Previous Studies in Labyrinth Weirs 22

CHAPTER THREE: MATERIALS AND METHODS 24

3.1 Materials 24

3.1.1 Experimental models 24

3.1.2 Laboratory Flume 25

3.1.3 Point gauge 26

3.1.4 Weighing scale 27

3.1.5 Stop watch 28

3.1.6 Pitot tube 28

3.2 Methods 29

3.2.1 Experimental setup 29

3.2.2 Weir Equation 30

3.2.3 Discharge coefficient 31

3.2.4 Hydraulic Weir Performance 31

3.2.5 Surface Profile Study 32

3.2.6 Dimensional Analysis for the Semi-Circular Weir 33

CHAPTER FOUR: RESULTS AND DISCUSSION 34

4.1 Results 34

4.2 Water surface Profile 34

4.3 Measured flow parameter on the semi-circular broad crested weir 37

4.4 Hydraulic performance of the semi-circular weir models 44

4.5 Developed Model Equations 45

4.6 Cost Implication 49

CHAPTER FIVE: CONCLUSIONS AND RECOMMENDATIONS

5.1 Conclusions **53**

5.2 Recommendation **54**

REFERENCES 55

APPENDIX **57**

APPENDIX A 57

APPENDIX B**:** Water depth for different discharge conditions 58

APPENDIX C**:** Water depth for discharges downstream the weir 59

LIST OF PLATES

Plate I:	side view of the Tilting Flume used for the study	26
Plate II:	A typical pointer gauge used for the study	27
Plate III:	Weighing machine placed at the receiving end of the tilting flume	28
Plate IV	L-pitot tube	29
Plate V:	Weirs of radius 5cm	57
Plate VI:	Weirs of radius 7.5cm	57
Plate VII:	Weirs of radius 10cm	57
Plate VIII:	Flow over normal weir	57
Plate IX:	Plan of normal weirs	57
Plate X:	Down stream flow	57

LIST OF FIGURES

Figure 2.1	The Cross-section Details of Sharp Crested Weirs	6
Figure 2.2	Schematic View of Flow over Weir	6
Figure 2.3	Relationship between C_d and $\frac{H}{P}$ for various α based on Borghei*et al.* (2003)	12
Figure 2.4	Relationship between C_d and $\frac{H}{P}$ for α = 30°, R = 5 cm with various P based on Noori and Chilmeran (2005)	14
Figure 2.5	Relationship between coefficient of discharge (C_d) and the upstream head to crest radius value $\left(\frac{H_w}{R}\right)$ for weir of diameter = 11 cm	16
Figure 2.6	Relationship between coefficient of discharge (C_d) and the upstream head to crest radius value $\left(\frac{H_w}{R}\right)$ for weir of diameter = 9 cm	17
Figure 2.7	Relationship between coefficient of discharge (C_d) and the head to radius value $\left(\frac{H_w}{R}\right)$ for weir of Diameter = 6.33 cm.	17
Figure 2.8	Relationship between average coefficient of discharge (C_d) and the diameter of cylindrical weir (D)	18
Figure 2.9	Relationship between average discharge coefficient (C_d) and angle of inclination (β) of oblique cylindrical weir.	18
Figure 2.10	Comparison between experimental data of present study and ancient studies of the flow depth at crest	20
Figure 2.11	Relationship between C_d and $\frac{H_t}{R}$ for trapezoidal labyrinth weirs for various α based onTullis et al. (1995) and Willmore (2004)	23
Figure 3.2	Schematic diagram of the semi-circular crested weir	30
Figure 4.1	Water surface profile for different discharges	35
Figure 4.2	Downstream water surface profile	35
Figure 4.3	Variation of sequent Depth with discharge	36
Figure 4.4	Variation of C_d with angle of inclination	43

LIST OF TABLE

Table 3.1: Weir Geometry 25

Table 4.1: Showing characteristics of downstream profile of the weir 37

Table 4.2a: Measured and calculated flow parameters for weir models (A1) with R = 5cm and $\alpha = 90^o$ 37

Table 4.2b: Measured and calculated flow parameters for weir models (A2) with R = 5cm and $\alpha = 60^o$. 37

Table 4.2c : Measured and calculated flow parameters for weir models (A3) with R = 5cm and $\alpha = 30^o$. 38

Table 4.2d: Measured and calculated flow parameters for weir models (A4) with R = 5cm and $\alpha = 15^o$. 38

Table 4.3a: Measured and calculated flow parameters for weir models (A_5) with R = 7.5cm and $\alpha = 90^o$. 38

Table 4.3b: Measured and calculated flow parameters for weir models (A_6) with R = 7.5cm and $\alpha = 60^o$. 39

Table 4.3c: Measured and calculated flow parameters for weir models (A_7) with R = 7.5cm and $\alpha = 30^o$ 39

Table 4.3d: Measured and calculated flow parameters for weir models (A_8) with R = 7.5cm and $\alpha = 15^o$. 39

Table 4.4a: Measured and calculated flow parameters for weir models (A_9) with R = 10cm and $\alpha = 90^o$ 40

Table 4.4b: Measured and calculated flow parameters for weir models (A_{10}) with R = 10cm and $\alpha = 60^o$ 40

Table 4.4c: Measured and calculated flow parameters for weir models (A_{11}) with R = 10cm and $\alpha = 30^o$ 40

Table 4.4d: Measured and calculated flow parameters for weir models (A_{12}) With R = 10cm and $\alpha = 15^o$ 41

Table 4.5: Values of parameters as a result of regression analysis 42

Table 4.6: Performance in terms flow magnification for the semi-circular crested weir models 44

Table 4.7: Actual Discharge and Discharges Calculated From Weir Equation Developed 46

Table 4.8: Actual C_d and C_{ds} Calculated From Weir Equations of C_d 47

Table 4.9a: Cost Analysis of Semi-Circular Weir 49

Table 4.9b: Cost Analysis of Sharp Crested Weir 49

ABBREVIATIONS AND SYMBOLS

A1-12: Model number

A_t: Area of Tank

B: Channel Width

b = weir width

B_1: Channel Width (Kindsvater and Carter (1957))

b_c: Width of the Weir (Kindsvater and Carter (1957))

b_e : Effective Width of the Weir

C : Calibration Constant

C_d : Discharge coefficient

C_{dH} : Coefficient of discharge based on full centerline weir length

C_{dw} = Coefficient of discharge determined by Noori and Chilmeran

C_e: Effective Discharge Coefficient

d_1 : Upstream flow depth

d_2: downstream flow depth

d_c : critical flow depth of the channel

d_{crest} : depth of flow measured at weir crest (m);

DE : drop in energy from point 1 to 2

E_1: energy at initial depth

E_2: energy at sequent depth

F_1: froude number at initial depth

F_2 : Froude number at sequent depth

Fr : Froude number

G: Acceleration due to gravity

h : Head above crest

H: Upstream piezometric head

h/p : Head to crest height ratio

H_1 : Head upstream of the weir (m);

h_1 : Head over Weir (Kindsvater and Carter (1957))

H_1 : Total Section 1 head

H_2 : Total Section 2 head

H_a: Head due to approach velocity

he : Effective Head on the Weir

H_{eff} : Effective head over the weir

H_t : Total upstream head

H_w/R : Head to crest radius ratio

K : Parameter for head discharge relationships based on Borghei et al

K_b : Quantity represents the effect of surface tension and viscosity

l : Characteristic length

L: Effective length of the weir

L_e: Effective weir length

P: Height of weir

P_1 : Weir Height (Kindsvater and Carter (1957))

P_{s1}: Section 1 pressure

P_{s2}: Section 2 pressure

Q : Discharge

Q: Discharge per unit length

Q_{act} : Actual discharge

q_s : Discharge per unit width passing over normal sharp crested weir

qw/qs: Flow magnification factor

Q_{in}/Q_{nc} : Magnification Factor

Q_{NC} : Discharge over normal semi-circular crested weir

Q_{NS} : Discharge obtained from British standard institute (1965).

Q_{th} :Theoretical discharge

q_w : Discharge per unit width (m3/sec/ m);

R : Radius of crest

R_e : Reynold number

$R_{ecritical}$: Critical Reynold's number Recritical

t : Time

t_1- t_3 : Three different trial time

t_{av} : average time

u : Average Velocity

u_1 : Average Velocity at Section 1

u_2 : Average Velocity at Section 2

u_T : Average Velocity

V : Characteristic Velocity

V_1 : Initial depth velocity

V_2: Sequent depth velocity

V_a: Approach velocity

W: Weber number

z_1 : Section 1 elevation

z_2 : Section 2 elevation

ν: Fluid kinematic viscosity

ρ: Fluid density

γ: Specific Weight

μ: Dynamic viscosity

σ: Surface tension

ABSTRACT

The overflow characteristics of semi-circular crested weir models were investigated. Twelve models were fabricated and tested. The models were categorized into two groups; normal weirs and oblique weir models. Both group of model had constant weir height and had the crest radius varied three times; 5cm, 7.5cm and 10cm. However, for the oblique weir, the oblique angle was varied three times; 60^o, 30^o and 15^o. From experimental results, it was observed that for normal weirs, the coefficient of discharge (C_d) increases with corresponding increase in head to crest height ratio (h/P). There were increases in C_d by 3.75%, 3.11% and 3.12% for 5cm, 7.5cm and 10cm normal weirs respectively. However, the oblique weirs showed corresponding increases of (C_d) with the increase of (h/P) values; while the highest C_d values were obtained with weirs of small oblique angle ($\alpha = 15^o$) for all crest radius tested. There were increases in C_d values by 0.4%, 4.8% and 4.86% as the oblique angle was varied from 90^0 to 60^0, $60^0$to 30^0 and 30^0 to 15^0 respectively. For normal weirs, the performance in terms of the discharge magnification factor (Q_{ac}/Q_{NS}) increases as (h/P) values increases. Hence, for all values of crest radius tested, normal weirs of semicircular crests had performance better than those of sharp crested weirs. While, for oblique weirs the performance in terms of the discharge magnification factor (Q_{ac}/Q_{NS}) increases with the increases in (h/P) values for all oblique weirs tested, hence, Weirs of small oblique angles give high discharge magnification factor and performance. Therefore, the model with radius 5cm and oblique angle 15^o was selected as the most efficient with a discharge coefficient and magnification factor of 0.885 and 1.326 respectively. Expression for determining the flow rate over the semi-circular weir was developed through dimensional and regression analysis respectively. Similarly, linear and non-linear equations for estimating the discharge coefficients of the weir models were developed. It was found that the flow rate equation developed had

correlation coefficient of 0.986 with maximum error of 1.4%. Also, the linear and non-linear equations developed had correlation coefficients of 0.664 and 0.574 with maximum errors of 33.5% and 42.6% respectively. Finally, the mathematical models developed for computing the discharge coefficient can be used for design of normal and oblique semi-circular crested weirs.

CHAPTER ONE

INTRODUCTION

1.1 PREAMBLE

Weirs are stable over flow structures built across rivers or channels to spill or divert water. Weirs are the most primitive, easiest and most accurate flow structures that have various uses (Nawzad et al., 2004). Weirs are often used for diversions and regulations of flow as well as discharge analysis and depth control in various field of engineering involving applications of canals, rivers and reservoirs. They are often used for free-flow conditions. A normal linear weir is commonly used in canal applications as a diversion structure, and is positioned normal to the direction of flow (Tingey, 2011).

Forms of weirs include; sharp-crested, broad crested, ogee crest and circular weirs respectively. However, the curvature for circular weirs gives it some outstanding characteristics over other forms of weir such as stable overflow pattern, passing of floating debris easily, lower cost of construction and easily designed when compared to ogee weir (Chanson and Montes, 1997).

In engineering applications (canal), a linear weir may not be able to convey the required discharge due to insufficient freeboard (difference between water height and channel depth). Discharges can be increased without a corresponding increase in upstream head by merely increasing the weir length. However, increasing the weir length is often difficult since increasing the channel width in most engineering applications is impractical. Therefore, the use of oblique weir is a reasonable solution (Tingey, 2011).

Furthermore, the discharge may also be influenced by the crest configuration. A quarter round broad crested weirs may give higher discharge for a given head than a sharp crested weir; a half

round broad crested weir may give better discharge than the quarter round broad crested weir or sharp crested weir (Tingey, 2011).

The influence of round crests of broad crested weirs on the flow characteristics were studied by Al-Tabatabie et al. (1986) and Abid Ali (1989). However, Aichel (1953) and Ibraheem et al. (1988) studied oblique sharp-crested weir in terms of performance. Hay and Taylor (1970), Darva (1971), Al-Hasson (1978) and Ibraheem (1983), studied laybrinth sharp-crested weirs of various shape extensively (Noori and Chilmeran, 2005).

Weirs under submerged and free flow conditions were studied by many researchers; Matthews (1963) introduced a theoretical concept to explain the influence of viscosity and surface tension on the discharge over round-crested weirs. Scale effects which are often a problem in hydraulic modeling of overflow structures were accounted for in the equation he proposed for C_d determination (Nawzad et al, 2004).

Ramamurthy (1993) studied the influence of downstream and upstream weir slopes on the discharge coefficient values for circular weir. Chilmeran (1996) investigated experimentally the influence of semicircular crests on discharge over normal and oblique weirs. Chanson and Montes (1998) investigated the behavior of cylindrical weirs due to the nature of flow. Al- Tikity (2000) studied the nature of flow over the rectangular half round crested weirs and compared with the result obtained under free flow for sharp-crested weirs. Smith (1959) studied the characteristics of embankment weir under free flow and submerged flow. Rao and Rao (1973) investigated the characteristics of hydrofoil weir under free and submerged flow. Al-Neima (1983) studied the effect of free as well as submerged flow conditions on discharge coefficient of oblique sharp crested weirs. Fitz and Hager (1998) studied hydraulics of embankment weirs with

side slopes (1V:2H) for both upstream and downstream under free and submerged flow. (Nawzad et al, 2004).

However, results from equations generated by Noori and Chilmeran (2005) did not correspond with the data from which it was derived from. Hence, the verification of the equation of discharge coefficient obtained by Noori and Chilmeran (2005) could not be achieved (Tingey, 2011).

In the light of Tingey (2011) observations, this study evaluates the characteristic of semi-circular crested weirs under laboratory pump flow with the aim of generating the weir and discharge coefficient equations.

1.2 Aim and Objectives of the Study

The aim of this research is to:

Develop a relationship between the upstream head and the discharge over the semi-circular crested weir.

The specific objectives of the study are to:

a) Establish a relationship between the discharge coefficient and the head over the weir crest, the crest height and radius of the semi-circular crest of the model
b) Compare the performance characteristics of the models based on the angle of inclination of the weir to the direction of flow.
c) Select the model that has the optimum crest radius for maximum discharge coefficient.

1.3 STATEMENT OF RESEARCH PROBLEM

The discharge coefficient varies with changing configuration of a compound weir as well as its angle of inclination in the direction of flow. These affect the overall performance of the weir in discharging water into hydraulic structures such as dams and irrigation channels. This and many other factors show that There is need to study the head-discharge relationship over the weir and the dependence of discharge coefficient on the height of water above weir crest, weir height, radius of circular crest, and angle of weir inclination (Richard, 1985).

1.4 Justification of Study

In crop irrigation, there is the need for water to be measured accurately. Discharge measurements in open channels are often difficult due to variation in velocity along the depth of channel as well as non uniform channel geometry. Weirs allow water measurements to be carried out as a function of depth of flow and weir geometry. Therefore, weirs present one of the easiest and most reliable methods of discharge measurements in canals and open channels (Allen and Dalton, 2002).

However, literature as well as documentation on discharge from broad crested and semi circular weirs are limited. Hence, physical models of broad crested weirs with semi-circular crest configurations were analyzed in this study.

1.5 SCOPE OF THE STUDY

This study will focus on investigating the flow characteristics over semi-circular broad crested weir experimentally. The experiments were conducted in hydraulics laboratory, Department of Water Resources and Environmental Engineering, Ahmadu Bello University Zaria.

CHAPTER TWO

LITERATURE REVIEW

2.1 Theoretical Consideration

The sharp crested weirs are vertical obstructions placed normal to the direction of flow; hence water passes over the weirs. The downstream edge of weirs should be inclined at an angle of 60° or 45° (Figure2.1). According to Chow (1959), a sharp crested weir is not only a measuring device for open-channel flow but also the simplest form of over-flow spill way; that is, the profile of the spillway was determined in conformity with the flow nappe shape over a sharp-crested weir. Parameters used to describe the weir are; B refers to channel width, b is the weir width, P refers to weir height and h refers to water head above the weir that is measured 3h - 4h away from the weir upstream. The weirs are classified based on the weir opening (b), examples include; full width weirs, fully Contracted and partially contracted weirs (Bos, 1989).

a. Fully contracted weirs have a weir width (b) of smaller than channel width (B), so that the weir is separated from the bed and side effects of the flow.
b. Weirs with weir width extending to the full channel width (b/B = 1.0) are often referred to as full width weirs or suppressed (Rehbock) weirs (Sisman, 2009).
c. Contracted weirs whose beds as well as walls are slightly affected are referred to as partially contracted weirs.

In order to obtain exact results, the discharge should be measured when the nappe of weir is aerated (Franzini and Finnemore, 1997: and Subramanya, 1986). That is the pressure for the upper and lower nappe of fluid should be atmospheric (Sisman, 2009).

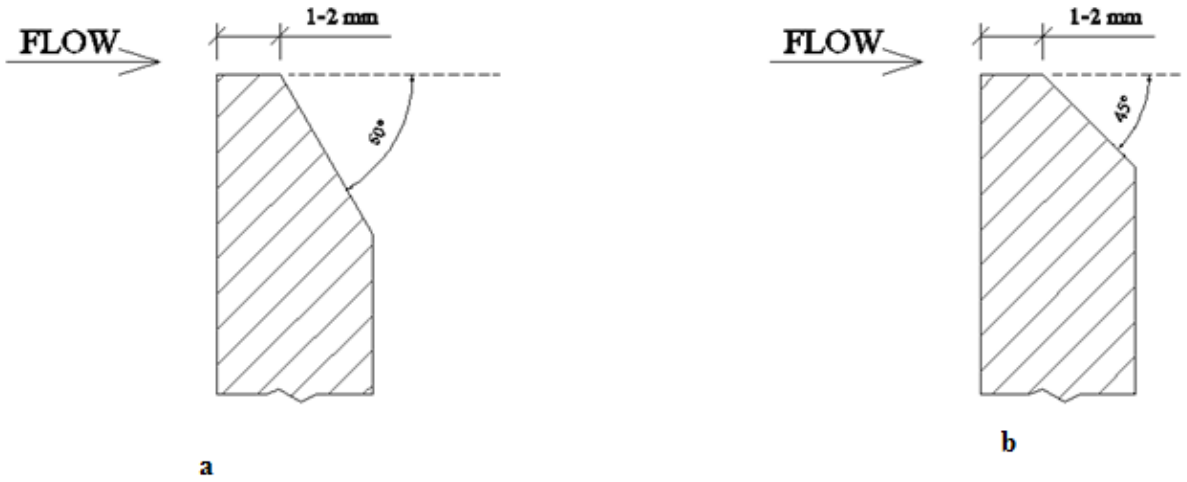


Figure 2.1**:** The Cross-section Details of Sharp Crested Weirs (Source: Sisman, 2009).

a Inclined angle of 60^o

b Inclined angle of 45^o

2.2. Discharge Equation

The theoretical discharge, Q_{ideal} for a rectangular sharp crested weir is found by assuming frictionless, parallel and horizontal flow with no loss (Henderson, 1966; Munson et al., 2002). Figure 2.2 shows a schematic view of flow over a sharp-crested weir.

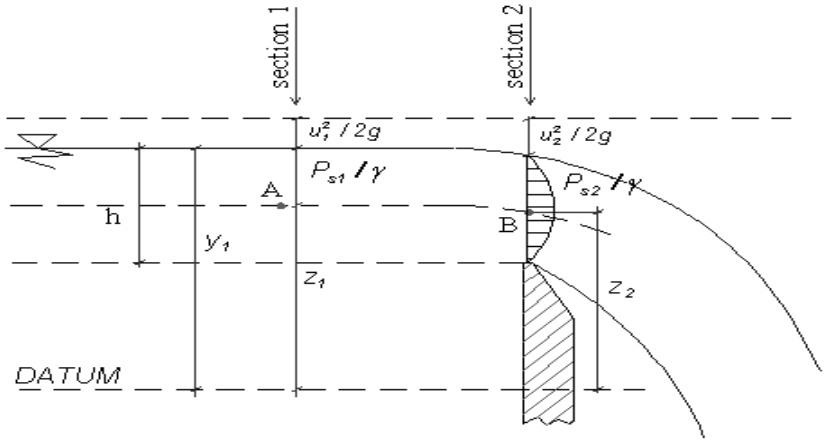


Figure 2.2 Schematic View of Flow over Weir (Source: Sisman, 2009).

Bernoulli equation for flow along an arbitrary streamline A-B in figure 2.2 can be written as:

$H_1 = H_2$ (2.1)

$\frac{P_{s1}}{\gamma} + Z_1 + \frac{U_1}{2g} = \frac{P_{s2}}{\gamma} + Z_2 + \frac{U_2}{2g}$ (2.2)

As can be seen from Figure 2.2, $\frac{Ps1}{\gamma} + Z_1 = y_1$, where y_1= upstream flow depth. The pressure over the weir is atmospheric such that $\frac{P_{s2}}{\gamma} = 0$

Thus the Eqn. (2.2) can be written as:

$Y_1 + \frac{U_1^2}{2g} - Z_2 = \frac{U_2^2}{2g}$ (2.3)

Then the velocity on the weir equals

$U_2 = \sqrt{2g(y_1 + \frac{U_1}{2g} - Z_2)}$ (2.4)

The discharge through an infinitesimal area element of depth δz for a weir width b is shown below $Q_{ideal} = U_2.b.\delta z$ (2.5)

Introducing equation (2.4) into equation (2.5) and integrating Q_{ideal} over z

$Q_{ideal} = \int_0^h \sqrt{2g(y_1 + \frac{U_2}{2g} - Z_2)}.b.\ \delta z$ (2.6)

$Q_{ideal} = \frac{2}{3}.b.\sqrt{2g}.b.\left[\left(h + \frac{U_1^2}{2g}\right)^{1.5} - \left(\frac{U_1^2}{2g}\right)^{1.5}\right]$ (2.7)

The velocity head at section 1 can be assumed negligible. Hence the equation of theoretical discharge is expressed as:

$Q_{ideal} = \frac{2}{3}.\sqrt{2g}\ .bh^{\frac{3}{2}}$ (2.8)

But the actual discharge, which depends on many parameters such as, geometry of weir, surface tension, viscosity and so on, is given below.

$Q = C_d\frac{2}{3}.\sqrt{2g}\ .\ bh^{\frac{3}{2}}$ (2.9)

2.3. Dimensional Analysis of a Sharp Crested Weir

Discharge passing over the weir is a function of several parameters (Figure 2.2), which are mathematically expressed by equation (2.10).

$$Q=f_1(h, b, B, P, \rho, \mu, g, \sigma) \quad (2.10)$$

A dimensional analysis is performed to find a relation between the discharge coefficient and other parameters stated above. Equation 2.11 gives a mathematical expression of this relation is given as follows;

$$\frac{Q}{g^{1/2} b h^{3/2}} = f_2\left(R, W, \frac{h}{b}, \frac{b}{B}, \frac{h}{P}\right) \quad (2.11)$$

Since the discharge equation can be expressed such that:

$$Q = C_d \frac{2}{3} \sqrt{2g}\ b h^{\frac{3}{2}} \quad (2.12)$$

Thus the discharge coefficient equals to:

$$C_d = \frac{Q}{2/3 (2g)^{1/2} b h^{3/2}} \quad (2.13)$$

Finally Equation (2.11) can be written as Equation (2.14). As can be seen, the discharge coefficient depends on Reynolds number, Weber number and geometry of weir and channel.

$$C_d = f_3\left(R, W, \frac{h}{b}, \frac{b}{B}, \frac{h}{P}\right) \quad (2.14)$$

For sharp crested rectangular weirs, measuring discharge accurately is very important. And since the discharge, which is needed to be found, depends on many parameters such as viscosity, surface tension and geometry, it is difficult to calculate the exact value of discharge. Several researches have been made to find an accurate equation of discharge coefficient (Sisman, 2009).

2.4 Weir Equation

The discharge coefficient of round-crested weir depends on both weir geometry and head. Because of the endless variety of weir shapes, however, no general solution for the discharge coefficient is available. One of the following methods is generally used to establish discharge coefficients for a particular weir (Harry, 1967):

i) Results of model tests for the particular dam used in the measurement.

ii) Comparison with other crest for which the discharge coefficient is known.

iii) Nappe-fitting method.

iv) Index-measurement method.

2.5 Previous Studies on Weir Equations

Henderson (1966) stated that for a normal sharp-crested weir, boundary-layer developments are found only at the vertical face of the weir due to low velocities. Hence, viscous effects are almost not associated with the flow. Also, if the weir crest runs the whole length of the channel, the flow will therefore be two-dimensional because the lateral contraction effects will be subdued by the channel sidewalls.

Assuming discharge over the weir is free of contraction; an elementary analysis can be made if it is also assumed that from the top of the weir to the water level the pressure is atmospheric. With the above assumptions, $\sqrt{2gh}$ represents the velocity at any point while h is the depth measured from the total energy line and q is discharge per unit width given by Equation (2.15) as

$$q=\int_{\frac{v^2}{2g}}^{H}\sqrt{2gh}\,dh=\frac{2}{3}\sqrt{2g}\left[H^{3/2}-\left(\frac{V^2}{2g}\right)^{3/2}\right] \quad (2.15)$$

The effect of the flow contraction expressed by a contraction coefficient C_c, is shown below

$$q = \frac{2}{3} C_c \sqrt{2g} \left[H^{2/3} - \left(\frac{V^2}{2g} \right)^{3/2} \right] \quad (2.16)$$

This can be compacted by introducing a discharge coefficient C_d making Eq. (2.16) become

$$Q = C_d \frac{2}{3} \sqrt{2g} H^{3/2} \quad (2.17)$$

Where

$$C_d = \left[1 - \left(\frac{V^2}{2g} \right)^{3/2} \right] \quad (2.18)$$

Finally, by multiplying Eq. (3) by the weir length, the standard weir equation is shown as

$$Q = C_d \frac{2}{3} \sqrt{2g} L H^{3/2} \quad (2.19)$$

The effects from placing the weir at an oblique angle were taken into consideration in the C_d calculation.

Rehbock (1929) made experiments of full width sharp crested weirs. And at the end of experimental works he concluded with a discharge coefficient equation which depends on water head on the weir (*h*) and weir height (*P*). The empirical equations of discharge and discharge coefficient are given in equations (2.19) and (2.20), respectively. (Rehbock, 1929)

$$Q = C_d \frac{2}{3} \sqrt{2g} b h^{3/2} \quad (2.20)$$

$$C_d = 0.611 + 0.08 \frac{h}{p} + \frac{1}{100} h \quad (2.21)$$

Rehbock's formula has been found to be accurate within 0.5% for values of *P* from 0.33 to 3.3 ft (0.1 to 1.0 m) and for values of *h* from 0.08 to 2ft (0.025 to 0.60 m) with the ratio *h/P* not greater than 1.0 (Franzini and Finnemore, 1997). The limitations of Rehbock's study were $0.10\ m \leq P < 1.00\ m$, $0.025\ m \leq h < 0.60\ m$, and $h / P < 1.00$

Kindsvater and Carter (1957) made an extensive study about sharp crested rectangular weirs. They introduced a parameter of C_e (effective discharge coefficient) which is free from the surface

tension and viscosity effects due to contraction of water at the weir (Equations 2.21, 2.22 and 2.23). The details of this study including results and limitations are explained in the following paragraphs.

In order to be consistent with equations and graphs, the symbols, Kindsvater and Carter used, are kept in their original form. The channel width *B* is shown as B_1, weir width *b* is shown as b_c, weir height *P* is $P_1$and water head on the weir *h* is $h_1$in this section (Sisman, 2009).

$$Q = C_e \frac{2}{3}\sqrt{2g} b_e h_e^{3/2} \quad (2.21)$$

$$C_e = 0.602 + 0.075 h_1/P_1 \quad \text{(full width weirs)} \quad (2.22)$$

$$b_e = b_c + K_b \quad (2.23)$$

$$h_e = h_1 + K_n \quad (2.24)$$

Where h_e=effective water height on weir

b_e = effective weir width

C_e = effective discharge coefficient

The quantities K_b and K_h represent several phenomena associated with surface tension and viscosity (Equations (2.22) and (2.23)). A recommended value of K_h = 0.001m was used for various ratios of $\frac{b_c}{B_1}$ and $\frac{h_1}{P_1}$. Equation (2.19) is actually a different form of actual discharge equation of sharp crested weir. The difference in equation (2.21) from equation (equation 2.19) is that weir width and water head are presented as a function of surface tension and viscous effects, they are not variables of discharge coefficient function (Sisman, 2009).

2.6 Previous Studies on Oblique Weirs

The foremost oblique weir investigation was attributed to Aichel (1953). He found an equation which showed the relationship at various angles of discharges for normal and oblique weirs.

$$\frac{q}{q_n} = 1 - \frac{H}{P}\beta_A \quad (2.25)$$

Where q is unit length discharge of the oblique weir, q_n is normal weir discharge per unit width of the weir and β is a coefficient dependent on α (Tingey, 2012).

Borghei et al. (2003) showed that for a small range of $\frac{H}{P}$, there exist a linear relationship between C_d and $\frac{H}{P}$ for oblique sharp-crested weirs at various angles. Figure 2.3. and Equation (2.25) show the relationship between C_d and H/P as suggested by Borghei et al. (2003), where the channel width over weir length (W/L) shows the effect of α (Tingey 2011).

$$C_{dH} = \left(0.701 - 0.121\frac{W}{L}\right) + \left(2.229\frac{W}{L} - 1.663\right)\frac{H}{P} \quad (2.26)$$

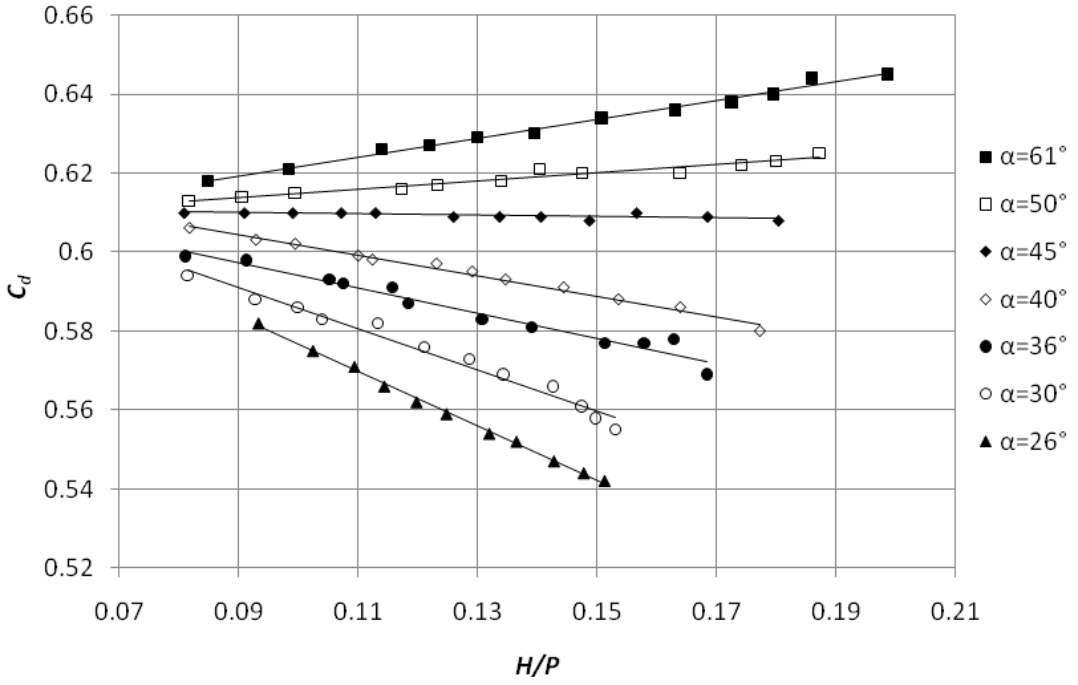


Figure 2.3: Relationship between C_d and $\frac{H}{P}$ for various angles based on Borghei*et al.* (2003)

(Source: Tingey, 2011)

Borghei et al. (2006) was able to generate four different head-discharge equations to describe the nature of flow for oblique sharp crested weirs, using incomplete self-similarity, considering the head over the weir downstream. Borghei et al. (2006) showed that Equation (2.26) to Equation (2.29) corresponded well with Borghei et al. (2003) than Equation (2.19) (Tingey, 2011).

$$\frac{H}{P} = 1.005\exp\left[0.277\left(\frac{L}{W}\right)\right]\left(\frac{K}{P}\right) \quad (2.27)$$

$$\frac{H}{P} = 0.982*10^{0.129(L/W)}\left(\frac{K}{P}\right)^{0.89\exp[0.09(L/W)]} \quad (2.28)$$

$$\frac{H}{P} = 1.34*10^{0.03(L/W)}\left(\frac{K}{P}\right)^{1.007} \quad (2.29)$$

$$\frac{H}{P} = \left[1.068 + 0.292\left(\frac{L}{W}\right)\right]\left(\frac{K}{P}\right)^{0.939+0.048(L/W)} \quad (2.30)$$

Where

$$K = \left(\frac{Q}{\sqrt{g}L}\right)^{2/3} \quad (2.31)$$

These equations are more difficult to use relative to Equation (2.25) and only provide minimal improvement in term of efficiency of prediction of results. Borghei et al. (2003) and Borghei et al. (2006) have limitation in the sense that their experimental data are limited to small $\left(\frac{H}{P}\right)$ values where velocity heads are minor (Tingey, 2012).

Noori and Chilmeran (2005) found that for normal and oblique weirs with semi-circular crest configuration of varying crest radius (R) of 5cm, 7.5 cm and 10 cm; varying weir height P of 20 cm, 25 cm, 30 cm; and varying oblique angle α of 30°,45°,60°, and 90°, the following relationship between C_{dw}, $\frac{H}{P}$, $\frac{R}{P}$, and α exist

$$C_{dw} = \frac{0.674}{(H/p)^{0.15}(R/P)^{0.54}(\sin\propto)^{0.86}} \quad (2.32)$$

To make C_{dw} comparable to C_d, the following operation can be performed

$$C_d = \frac{W}{L}\frac{3}{2\sqrt{2}g}C_{dw} \quad (2.33)$$

For oblique weirs with semi-circular crest configuration, Noori and Chilmeran (2005) found that given R, the discharge coefficient varies with P, as illustrate in Figure 2.4 (Tingey, 2011).

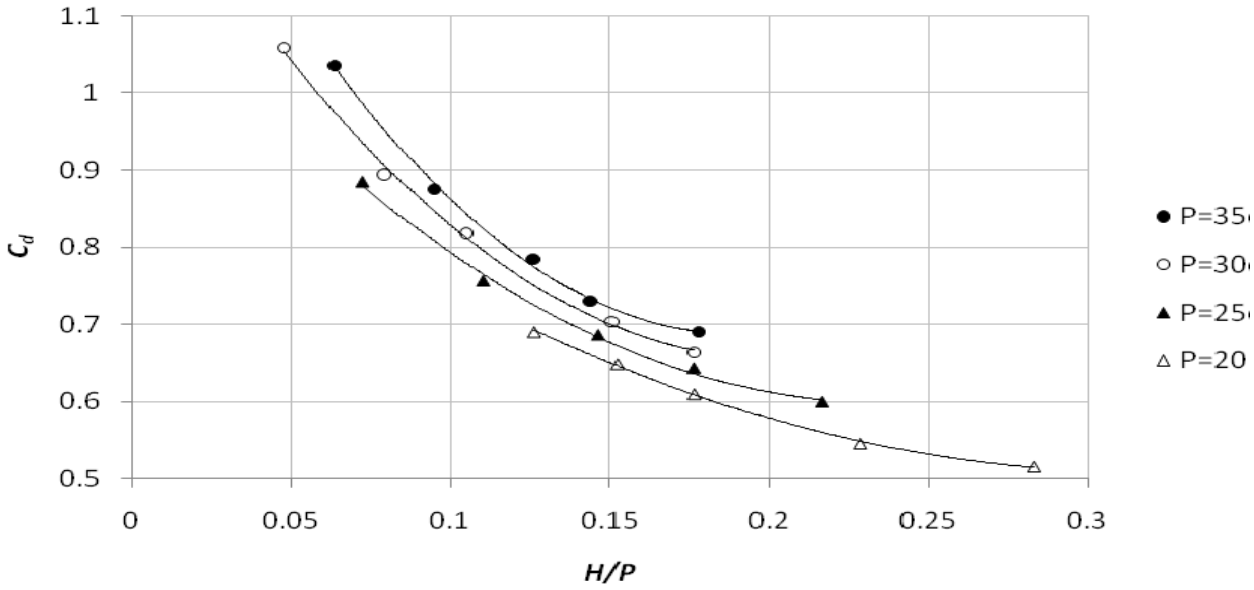


Figure 2.4 Relationship between C_d and $\frac{H}{P}$ for α = 30°, R = 5 cm with different P based on Noori and Chilmeran (2005). (Source: Tingey, 2011)

De Vries (1959) experimentally determined C_d for oblique and normal trapezoidal or dike form weirs with α = 30°, 45°, 60°. The C_d results were compared by Wols et al. (2006) and Uijttewaal (2007) with results obtained for numerical model of submerged oblique trapezoidal weir. The numerical model and De Vries' data showed good correlation between themselves. Though, Uijttewaal (2007) extended this study to include submerged objects that act as oblique weirs, Wols et al. (2006) actually developed the model(Tingey, 2011).

Tuyen (2006) determined C_d for an oblique trapezoidal weir. He found C_d values for oblique sharp-crested and broad crested weirs set at α = 45° and he also found that the C_d data compared well with that of Borghei et al. (2003) and De Vries (1959) (Tingey, 2011).

Crest shape influence on rectangular side weirs performance were studied by Noori and Jafar. Several crest shapes were studied and they observed that the side weir energy difference could be ignored because it is less than a percent. The discharge coefficient (CM) and upstream water depth to weir height ($\frac{h_1}{P}$) were correlated and a linear relationship was found for both. (CM) was

found to vary linearly with upstream Froude number (Fr_1). Furthermore, higher performance was obtained for small weir heights, for crest shapes considered. The highest performances for both inside semicircular crest and outside semicircular crest were determined at (r) = 3.15cm and (r) = 3.75cm, respectively. While, the highest performance for all the models was observed at (r) = 2.5cm and (r/p) = 0.25 (Noori and Jafar, 2011).

The experimental study and analysis of influence of the geometrical characteristics, of the oblique cylindrical weir on coefficient of discharge were studied by Al- Babely (2012). Three weir sizes were used and two angles for the deviation were considered. The experiments on cylindrical weir were performed by separating it into three groups. The first group used three sizes of weirs (11 cm, 9 cm, and 6.35 cm) and (90^o) angle (normal weir) with channel wall. The second and third groups include the use of the same diameter sizes used in the first group with (45^o, 30^o) angles (oblique weir) respectively. Throughout these experiment, the data for water depth above the standard rectangular sharp crested weir (h) were taken to calculate the discharge of the equation and the depth of water upstream the circular weir under study. In the case of vertical and oblique weirs (d_1), Al-Babely (2012) presented effect of selected factors on discharge coefficient as follows;

Influence of Upstream Head on Coefficient of Discharge

The graph of coefficient of discharge (C_d) against $\left(\frac{H_w}{R}\right)$ is illustrated in figures (2.5 to 2.7).These figures show that (C_d) is proportional to$\left(\frac{H_w}{R}\right)$. Also it was noticed that (C_d) is greatly affected by the upstream head over the crest (H_w). Where (C_d) values increase with increasing (H_w). It's apparent that at very low values of (H_w), the surface tension and viscosity effects would influence the behavior and results in curves shown in figure 2.5.

Effect of diameter of weir on discharge coefficient

The effect of diameter of weir was investigated through series of experiments. The average discharge coefficient for each model is plotted against diameter of weir as shown in the figure (2.8). It is obvious that the discharge coefficient decreased as the diameter of weir increased. The sufficient increase in acceleration or centrifugal forces in the flow direction is due to effect of curvature. It appears that if the stream lines are curved there is a significant flow velocity that leads to increases in the discharge coefficient.

Effect of weir inclination on flow

The coefficient of discharge (C_d) and weir inclination with channel wall (β) was plotted as shown in figure (2.9). It was noticed that the average (C_d) was inversely proportional to (β). This means that the oblique weir has higher (C_d) than the vertical weir. Weir of oblique angle (β) = 30° gave the highest values of (C_d) when compared to those of 45° and 90° because longer weirs length are obtained with weirs of small oblique angle.

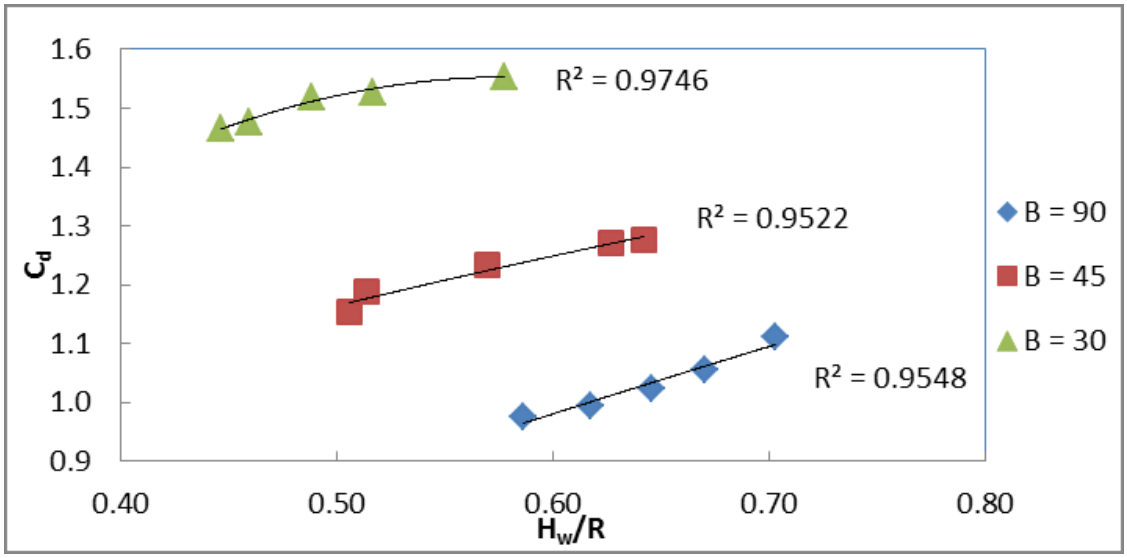


Fig. 2.5 Relationship between discharge coefficient (C_d) and the dimensionless Value $\left(\frac{H_w}{R}\right)$ for weir of diameter = 11 cm. (Source: Al-Babely, 2012)

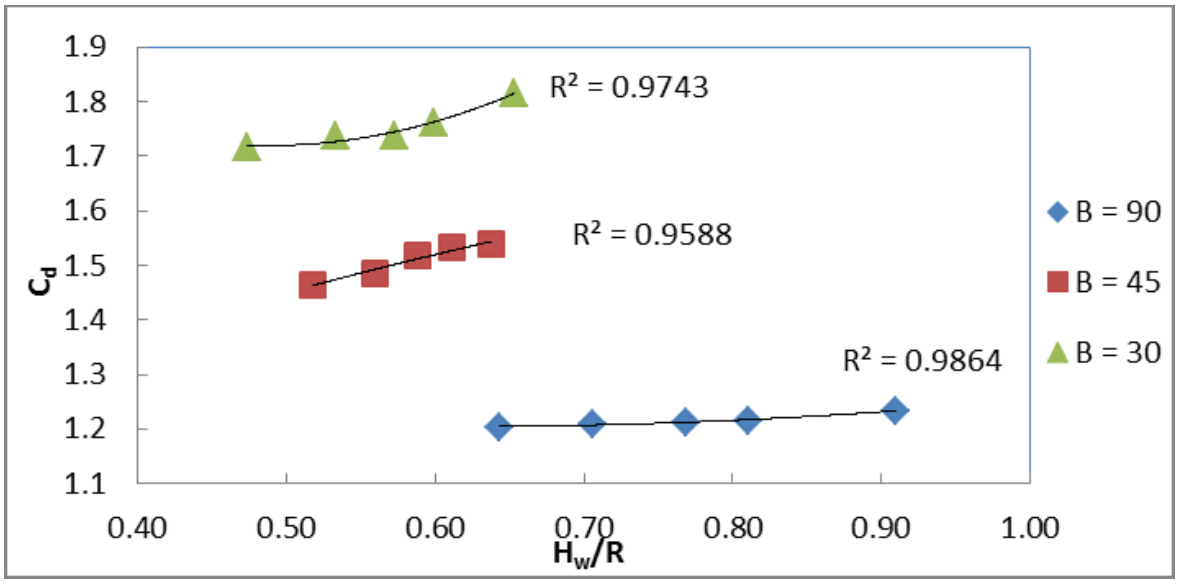


Fig. 2.6 Relationship between coefficient of discharge (C_d) and the $\left(\frac{H_w}{R}\right)$ Values

For weir of diameter = 9 cm. (Source: Al-Babely, 2012)

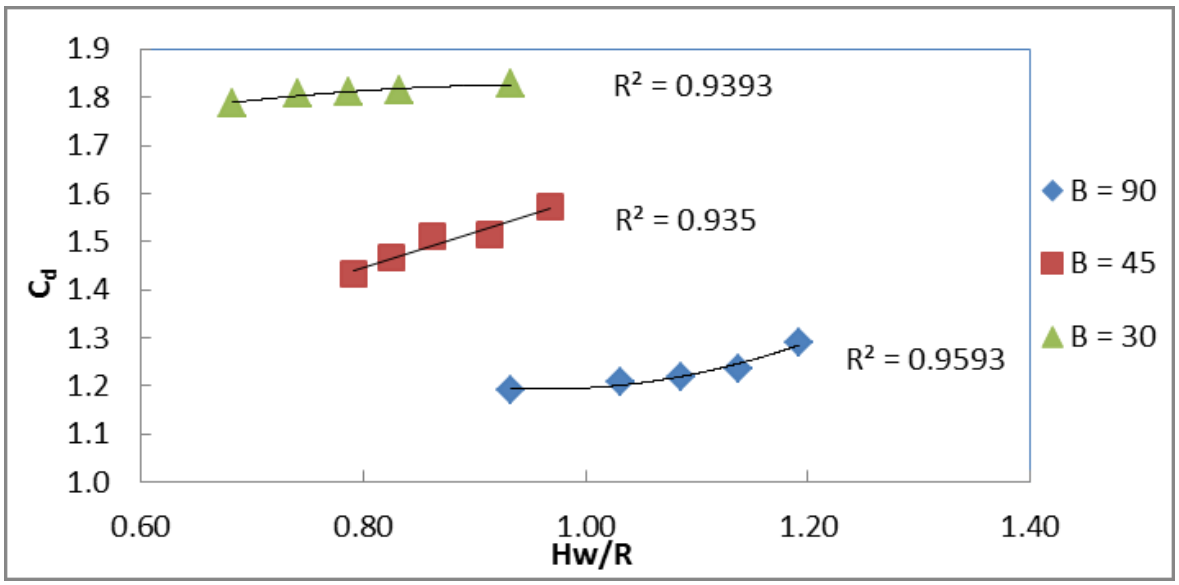


Fig.2.7 Relationship between coefficient of discharge (C_d) and $\left(\frac{H_w}{R}\right)$ value

for weir of Diameter = 6.33 cm. (Source: Al-Babely, 2012)

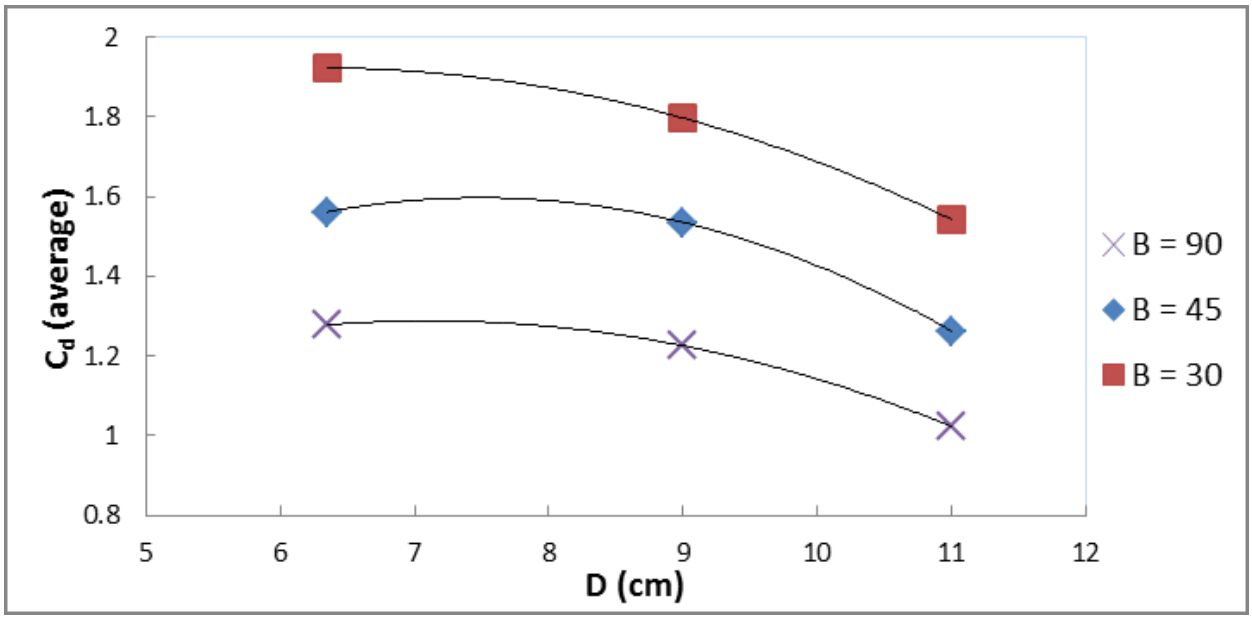


Fig. 2.8 Relationship between average coefficient of discharge (C_d) and the diameter of cylindrical weir (D). (Source: Al-Babely, 2012)

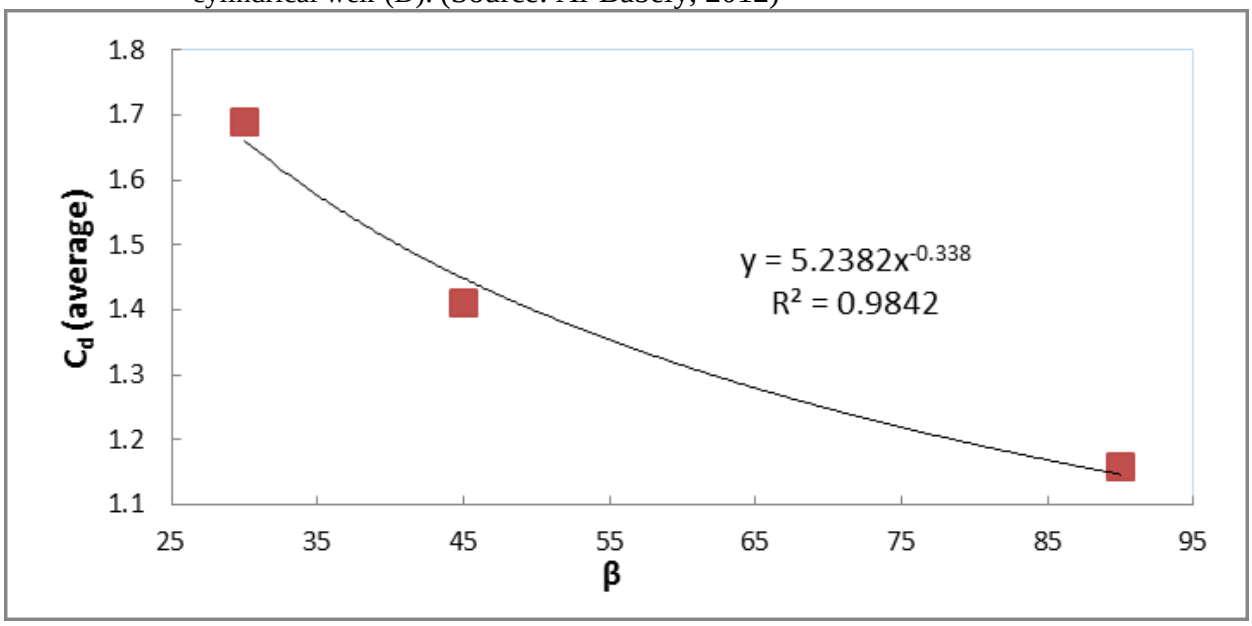


Fig. 2.9 Relationship between average coefficient of discharge (C_d) and the angle of inclination (β) of oblique cylindrical weir. (Source: Al-Babely, 2012)

From the results, it was found that the discharge coefficient is influenced by geometrical characteristics represented by radius of the weir and the angle of inclination with the wall of the channel. It was found that the increase in the radius of the weir lead to a low coefficient of

discharge of the cylindrical weir. More so, the coefficient of discharge of the oblique weir is higher than the coefficient of discharge of the normal weir. However, it was found that the coefficient of discharge value was directly proportional with the weir inclination.

The flow characteristics of cylindrical normal weirs were experimentally studied **by** Al Babely et al (2011). The result they obtained showed that for the same weir height, increases in the head to weir radius ratio $\left(\frac{H_w}{R}\right)$ values lead to increases in coefficient of discharge (C_d) value. Therefore, they noted that the radius of cylindrical weir (R) had influence on (C_d). The performance in terms of flow magnification factor (qw/qs) increases with an increase in $\left(\frac{H_w}{R}\right)$. It is worth noting that, although Chanson and Montes (1998) data were obtained with fully developed inflow conditions, their measurements show the same trend as the present study, and VO(1992) data (figure 2.10).

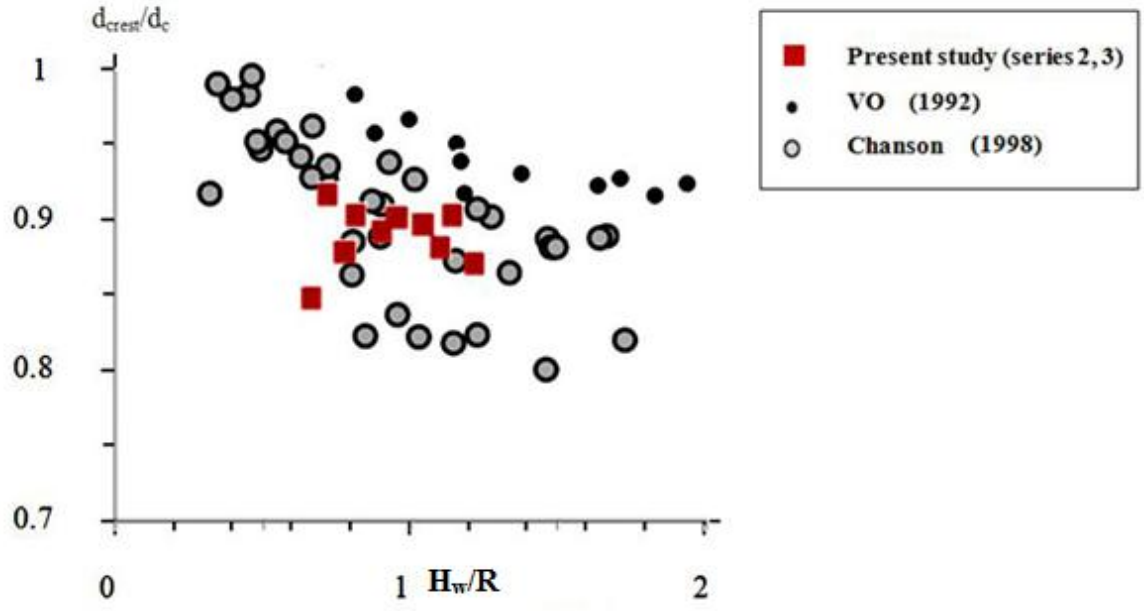


Fig. 2.10: Comparison between experimental data of present study and ancient studies of the flow depth at crest. (Source: Al-Babely, 2012)

Furthermore, the data of present study, and both VO and Chanson (1998) indicated that $\frac{d_{crest}}{d_c}$ is less than one for $H_w/R > 0.5$. The flow magnification factor $\left(\frac{q_w}{q_s}\right)$ was plotted against $\left(\frac{H_w}{R}\right)$ in figure 7 for different values of crest radius (R = 5.7 cm, 4.5 cm, 3.15 cm). From this figure, one can conclude that though $\left(\frac{q_w}{q_s}\right)$ increases with increase in $\left(\frac{H_w}{R}\right)$ value, the magnification factor for all ranges of $\left(\frac{H_w}{R}\right)$ were greater than unity. The result of the whole study may be summarized as:

1. Water surface profiles for all weirs were smooth and continuous showing a descending trend with a steep drop near the downstream face of the weir.
2. The water surface profiles became horizontal at distance (6.3 – 11.2) h. This is the suitable location where a point gauge should be located for accurate measurements of upstream water head.
3. The relationship between coefficient of discharge (C_d) and head to weir radius ratio $\left(\frac{H_w}{R}\right)$ was found. For the same weir height, the increase in head to weir radius ratio $\left(\frac{H_w}{R}\right)$ lead to increase in the value of (C_d).
4. The flow magnification factor $\left(\frac{q_w}{q_s}\right)$ increases with increase in $\left(\frac{H_w}{R}\right)$ and for all values of $\left(\frac{H_w}{R}\right)$, the magnification factor were greater than one.
5. The cylinder face downstream showed nappe adherence at low to medium overflows (0.009 to 0.012)$m^2/2$, and rapid flow redistribution upstream of the cylindrical weir.
6. For the range of the experiments, the radius of cylindrical weir was observed to have effects on the discharge coefficient.
7. The study showed that the critical depth (d_c) is normally higher than the flow depth at weir crest (d_{crest}), and $\frac{d_{crest}}{d_c}$ is typically about 0.85 (Al Babely et al., 2011).

The coefficients of discharge for oblique weirs were studied by Tingey (2011). These included sharp crested, semi-circular crested and quarter-round-crested weirs. The quarter-round -crested weirs performed more efficiently than the sharp crested weir and semi-circular crested weirs were more efficient than both the quarter-round and sharp crested weirs (Tingey, 2011).

The characteristics of compound crested weir models were investigated experimentally by Muhammad (2012). The crests of these weir models consist of two parts; the upstream part has a quarter round shapes while the downstream part has standard sharp crested weir shape. Series of experiments were conducted by measuring discharges and water heads over the weir models for various weir crest radii of R = 2.5cm, 3.5cm, 4.5cm and angles of weir inclination $\alpha = 30^o$, 45^o,60^o, 90^o to the direction of flow with a constant weir height of P = 15cm. It was observed that the increase in the ratio of water head above the crest (h) to weir height (P) resulted in the corresponding increase in the discharge coefficients for all the weir models. The hydraulic performance for each of the weir was determined in terms of the flow magnification factor. Hence, the model with R = 2.5cm and $\alpha = 30^o$ was selected as the best model because it had the highest discharge coefficient and flow magnification factor of 1.326 and 1.555 respectively. Expression for determining the flow rate over the compound crested weir models was developed through dimensional and regression analysis respectively. Similarly, linear and non-linear equations for estimating the discharge coefficients were developed where it was found that the flow rate equation developed had correlation coefficients of 0.714 with maximum error of 1.98 percent. Also the linear and non-linear equations developed for predicting the discharge coefficients had correlation coefficients of 0.880 and 0.926 with maximum errors of 9.41 percent and 5.45 percent respectively.

Salmasi et al (2012) investigated the influence on coefficient of discharge (C_d) by lower weir crest width as well as step height associated with rectangular compound cross section of broad-crested weirs and coefficient of approach velocity. Because the section width suddenly changes shape, a discontinuity was observed in the head-discharge curve. More so, Salmasi et al (2012) observed that due to contraction effects the C_d values of the broad-crested compound weir were lower than that observed for broad crested weir with rectangular crest configuration (Salmasi et al.,2012).

2.7 Previous Studies in Labyrinth Weirs

Labyrinth weirs refers to weirs that appear folded in plan view. They may have crest profiles ranging from triangular, rectangular to trapezoidal. Figure 2.11 shows a cycle of each labyrinth weir type.

Tullis et al. (1995) was able to determine a relationship between C_d and $\frac{H_t}{P}$ for $\alpha = 6°$ to $35°$ for quarter round crests trapezoidal labyrinth weir from C_d measurement carried out.

Willmore (2004) corrected results obtained for the trapezoidal labyrinth weir of quarter round crest configuration with $\alpha = 8°$. A 10° labyrinth weir curve was interpolated between Tullis el al. (1995) 12° data and Willmore 8° data. It was observed that the interpolated curve could be compared with the 10° oblique quarter round crest data. More so, it was observed that comparisons could also be made between quarter round crested oblique weirs and the 15° and 25° labyrinth weirs (Tingey, 2011).

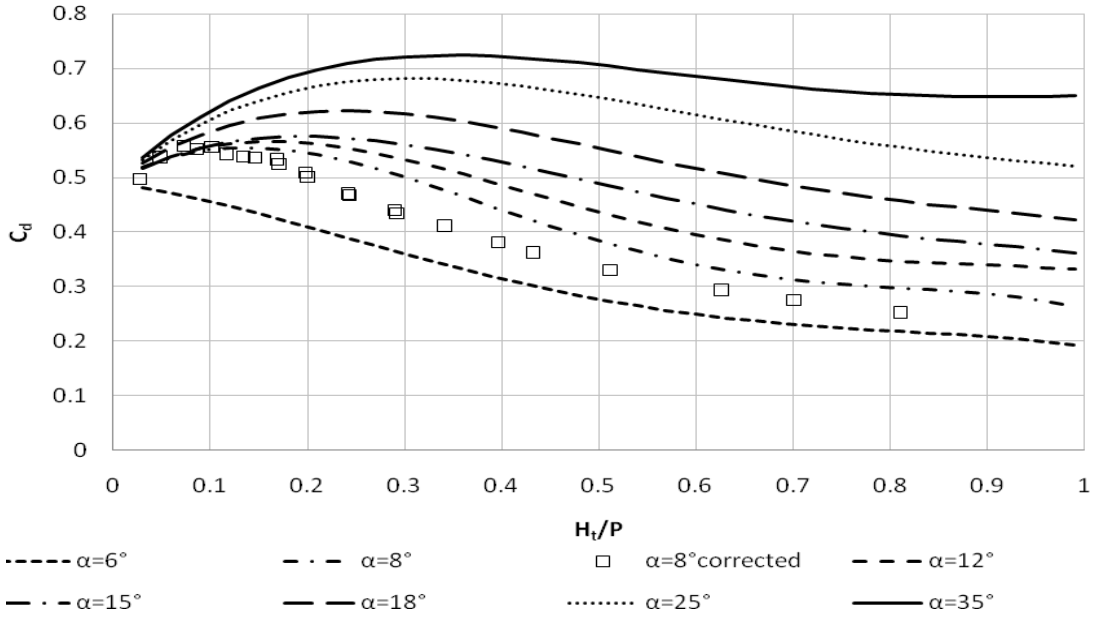


Figure 2.11: Relationship between C_d and $H_t \frac{H_t}{P}$ for trapezoidal labyrinth weirs of different α based on Tullis et al. (1995) and Willmore (2004). (Source: Tingey,2011)

Wilmore (2004) also measured C_d experimentally for semi-circular crested trapezoidal labyrinth weirs. 25° labyrinth weir was interpolated and compared it with the 25° semi-circular crested oblique weir.

The discharge capacity may be reduced due to the presence of labyrinth weir apexes, because the weir length became less or ineffective.

Tullis et al.(1995) replaced the entire weir length in the weir equation (2.19), when determining Q and C_d with effective length L_e . Ineffective regions were observed where oblique weirs meet the channel wall which was similar to the ones observed for labyrinth weir (Tingey, 2011).

CHAPTER THREE

MATERIALS AND METHODS

3.1 Materials

The following materials were used in this work.

3.1.1 Experimental Models

The physical model was fabricated from wood with a configuration of a semi-circular crest as shown in figure 1, the radius was determined according to the design criteria suggested by Abid-Ali (1986), in which the radius of the weir (R) should at least equal to the weir height (P) divided by 12.

$$R = {}^{P}/_{12} \tag{3.1}$$

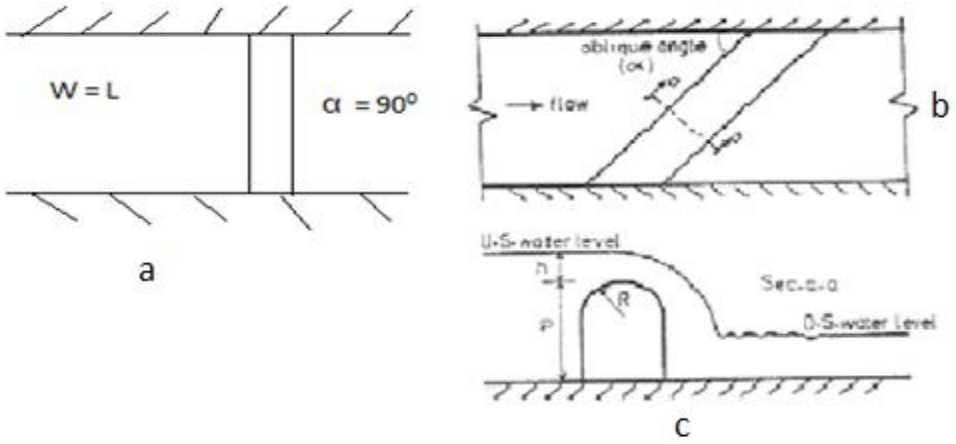


Figure 3.1: Schematic diagram of the semi-circular crested weir

A plan view of a semi-circular crested weir

B plan view of an oblique semi-circular crested weir

C side view of a semi-circular crested weir.

The experimental work were conducted on twelve (12) different fabricated models with angles of inclination to the direction of flow $\alpha = 15^o$, 30^o, 60^o and 90^o and for different discharges. A summary of the weir geometries tested is given in Table 3.1

Table 3.1: Weir Geometry

Model No.	**Group No.**	**Oblique Angle(α)**	**Series No**	**Crest Radius R(m)**	**Effective Crest Length L(cm)**	**Crest Height P(cm)**
1 2 3	1	90^o (Normal weir)	A B C	5.0 7.5 10.0	30.0 30.0 30.0	20
4 5 6	2	60^o	A B C	5.0 7.5 10.0	34.6 34.6 34.6	20
7 8 9	3	30^o	A B C	5.0 7.5 10.0	60.0 60.0 60.0	20
10 11 12	4	15^o	A B C	5.0 7.5 10.0	115.9 115.9 115.9	20

3.1.2 Laboratory Flume

The experiment was conducted in a rectangular laboratory tilting flume of length 6 meter, 0.3 meter wide and 0.3 meter deep (plate I). The flume has rails on top of its glass-sided walls on which a pointer-gauge trolley was moved to and fro for the measurement of water depths. It also had a tailgate located at its outlet end to regulate the downstream water depth to the desired depth so that hydraulic jump can occur at downstream toe end of the inserted models. The flume have a continuous flow pumping mechanism, a control valve for regulating the pumped water

flow from its storage tank into the rectangular channel of the flume, a stilling storage provisions at the downstream end of the flume channel and flow measuring facilities to measure the regulated flow through its channel at any time. The flume measures discharge in terms of mass flow rate which was converted to volumetric discharge by dividing with the density of water.



Plate I: side view of the Tilting Flume

3.1.3 Point gauge

Water depth as well as the height above the crest was measure during the experiments using an accurate point gauge (plate ii). The point gauge was used to ensure that P for each weir was constant because of the thickness of carpenter's putty used and variations in installation. The measurement of height above the crest was taken with the point gauge located in accordance to Subramanya (1986) and Franzini and Finnemore (1997), the effective measurement point is

considered as 3-4h away from the weir location in order to get rid of draw down effects. Where h is the head of above weir crest.



Plate II**:** A typical pointer gauge used for the study

3.1.4 Weighing Scale

The mass flow rate over the weir was measured with the aid of a weighing scale which was attached to the receiving end of the flume (plate III).

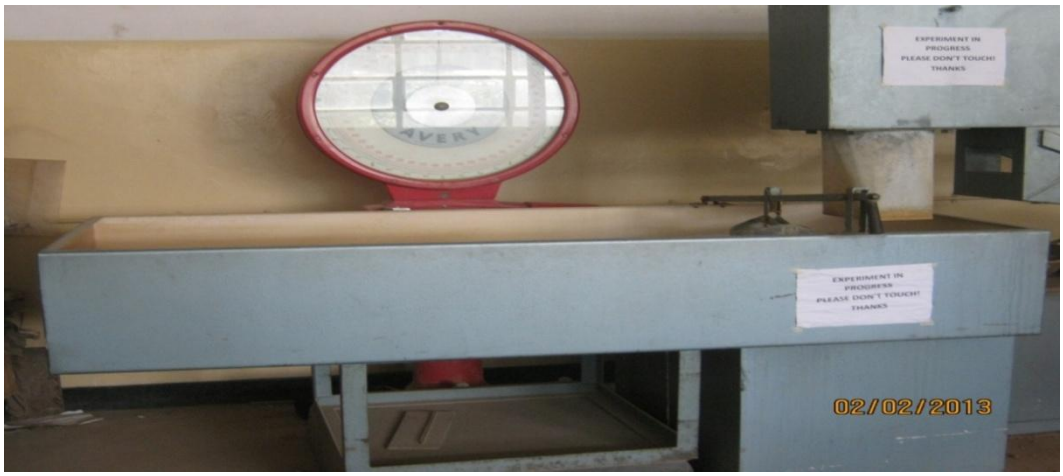


Plate III**:** Weighing machine placed at the receiving end of the tilting flume

3.1.5 Stop watch

Stop watch was used to obtain the time required to get certain amount of water flowing over the weir in other to ascertain the discharge over the weir.

3.1.6 Pitot tube

The velocity upstream and downstream of the weir was measured with the aid of a pitot tube (plate IV). This will enable a good estimation of the discharge.



Plate IV**:** Pitot tube

3.2 METHODS

3.2.1 Experimental Setup

A moveable point gauge was used to measure the downstream and the upstream water surface profile as well as measuring crest height of the models. A centrifugal pump was used to circulate water through the flume. Twelve models were produced and tested. The models were categorized into four groups depending on the oblique angle (α). A constant weir height (P) was used for all models in each group with the crest radius (R) varied from 5cm, 7.5cm to 10cm. The groups consisted of the normal weir (90^o), the 60^o, 30^o and 15^o oblique weirs respectively. Though all models were polished and varnished to give smooth surfaces, they were produced from wood. Each model was placed 3.5m from the inlet of the flume and various discharge were passed over

the weir model. Six different discharges were passed over each model and the heights of water over specific grid point were measured in order to determine the upstream and downstream surface profiles.

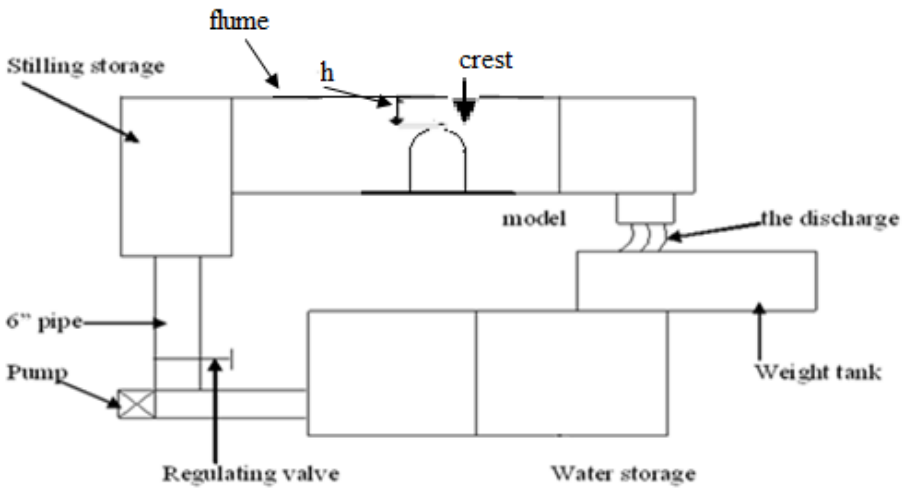


Figure 3.2: Schematic representation of the experimental set-up.

3.2.2 Weir Equation

Since the physical model is considered to belong to the rectangular broad crested weir, the proposed theoretical equation for the normal and inclined semi-circular crested weirs was initially assumed to be the basic equation developed for the linear weirs according to Chow (1959), expressed as Equation (3.2).

$$Q = \frac{2}{3} C_d L \sqrt{2g} h^{3/2} \quad (3.2)$$

However, the discharge equations as well as the discharge-coefficient equations were generated from the regression analysis of the results obtained from the physical model.

3.2.3 Discharge coefficient

Regression analysis was performed between he measured discharges 'Q', the head of water above crest 'h' and the angle of weir inclination 'α' in order to arrive with a relationship in the following format of equation, as suggested by Muhammad (2012).

$$Q = \frac{CH^n}{sin\propto^m} \quad (3.3)$$

Where c, n and m are parameters to be estimated by regression analysis.

Therefore the discharge coefficient, $C_{d,}$ has been taken as the ratio of the actual discharge, Q_{act}, to the theoretical discharge Q_{theo} given by:

$$C_d = \frac{Q_{act}}{Q_{theo}} \quad (3.4)$$

The actual discharge (Q_{act}) was measured using gravimetric method which was converted to m^3/s using the equation below.

$$Q_{act} = \frac{M}{\rho t_{av}} \quad (3.5)$$

Where

$$Q_{theo} = \frac{2}{3} L\sqrt{2g}h^{3/2} \quad (3.6)$$

$$L = \frac{B}{sin\propto} \quad (3.7)$$

3.2.4 Hydraulic Weir Performance

The hydraulic performance for normal weirs and oblique weirs was represented in terms of magnification factor defined as the ratio of discharges over normal weir of semi-circular crest

(Q_{NC}) and an imaginary normal sharp crested weir of the same height (Q_{NS}). The discharge over an imaginary sharp crested weir were determined from relevant equation recommended by the British Standard Institute (1965) (BSI 1965) (Noori and Chilmeran, 2005).

However, the magnification factor for oblique weirs is the ratio of discharges over oblique weir with semi-circular crest and normal weir with semi-circular crest (Noori and Chilmeran, 2005).

3.2.5 Surface Profile Study

In order to decide the point gauge location, water surface profile was made for different discharge values. Water depth was recorded for different discharges and a graph was used to illustrate water surface in the channel of the flume. The x-axis of the graph represented the distance from the weir while the y-axis represented the water height from the bottom of the channel.

3.2.6 Dimensional Analysis for The Semi-Circular Weir

A functional relationship was developed using dimensional analysis based on the idea of Noori and Chilmeran (2005), that the overflow characteristics of semicircular crested oblique weirs can be expressed as follows;

$$q = \varphi_1 (h, P, R, g, \alpha) = 0 \quad (3.8)$$

The general relationship among all variables is:

$$\Phi_2 (q, h, P, R, g, \alpha) = 0 \quad (3.9)$$

From dimensional analysis Equation (3.9) can be written as

$$\frac{q}{\sqrt{g}h^{3/2}} = C_d = \Phi 3 \left(\frac{h}{P}, \frac{R}{P} \sin \alpha \right) \quad (3.10)$$

In which the discharge coefficient is expressed as a function of ratios of; head to crest height, crest radius to crest height and sine of angle of inclination (Noori and Chilmeran, 2005).

CHAPTER FOUR

RESULTS AND DISCUSSION

4.1 Results

Seventy-two experiments were conducted in the hydraulics laboratory to determine flow parameter namely water surface profile, head of water above the crest 'h', actual discharge $Q_{act,}$ theoretical discharge Q_{the}, and discharge coefficient C_d. The Tables 4.2(a-d), 4.3(a-d), and 4.4(a-d) show the various values of h, Q_{act} and Q_{the} based on various crest radius R= 5cm, 7.5cm, and 10cm respectively. Each of these crest radius consist of four different angles of inclination to the direction of flow (that is $\propto = 15^o, 30^o, 60^o$ and 90^o).

4.2 Water surface Profile

The graph in Figure 4.1 illustrates the water surface profile upstream of the weir using the measured water depth in Appendix B for seven various discharges Q_1 to Q_7 (2.143 to11.765 (l/s)). The water surface is virtually stationary at 0.5m from the weir. At this point, it appears that the depth becomes linearly dependent on the discharge. Hence, the point gauge could be placed at that point to measure the respective head above the crest for different discharges. However, the point gauge was placed at 0.70m in accordance to section 3.1.3 of the methodology.

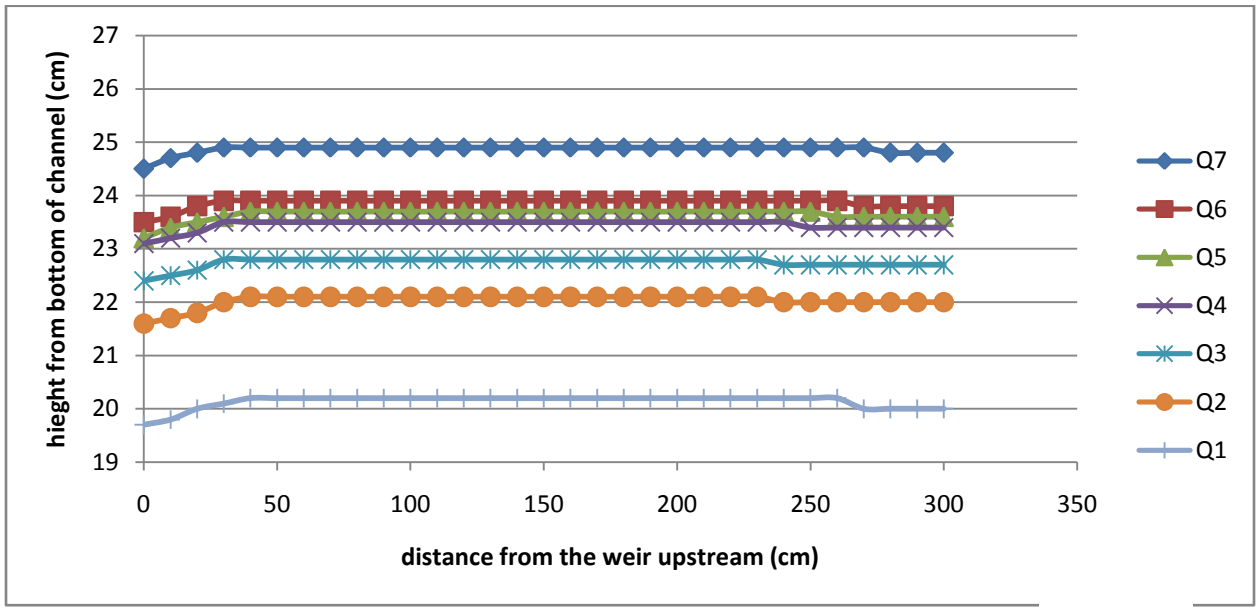


Figure 4.1**:** Water surface profile for different discharges

The graph in figure 4.2 illustrates the downstream water surface profile using the water depth in Appendix C for the same seven discharges considered in Appendix B.

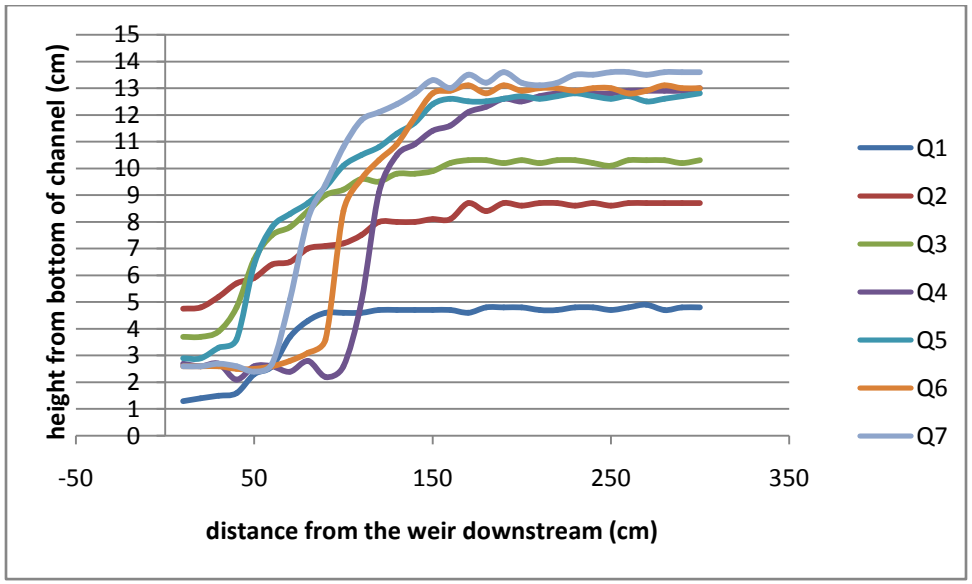


Figure 4.2: Downstream water surface profile

Table 4.1**:** Characteristics of downstream profile of the weir

discharge Q	values of Q (l/s)	initial depth Y_1 (cm)	sequent depth Y_2(cm)	V_1 (m/s)	V_2 (m/s)	f_1	f_2	E_1 (m)	E_2 (m)	DE (m)	efficiency
Q1	2.143	1.6	4.8	1.421	0.392	3.587	0.571	0.118	0.056	0.062	0.473
Q2	5.660	4.8	8.7	1.63	0.416	2.375	0.450	0.182	0.096	0.086	0.526
Q3	7.212	3.7	10.3	1.65	0.421	2.739	0.419	0.174	0.112	0.062	0.642
Q4	10.601	2.8	12.6	1.75	0.44	3.339	0.396	0.183	0.136	0.047	0.744
Q5	11.029	3.6	12.6	1.84	0.58	3.096	0.522	0.207	0.143	0.064	0.691
Q6	11.194	3.1	12.9	1.941	0.43	3.520	0.382	0.221	0.138	0.083	0.626
Q7	11.765	2.7	13.5	2.16	0.791	4.197	0.687	0.262	0.167	0.096	0.635

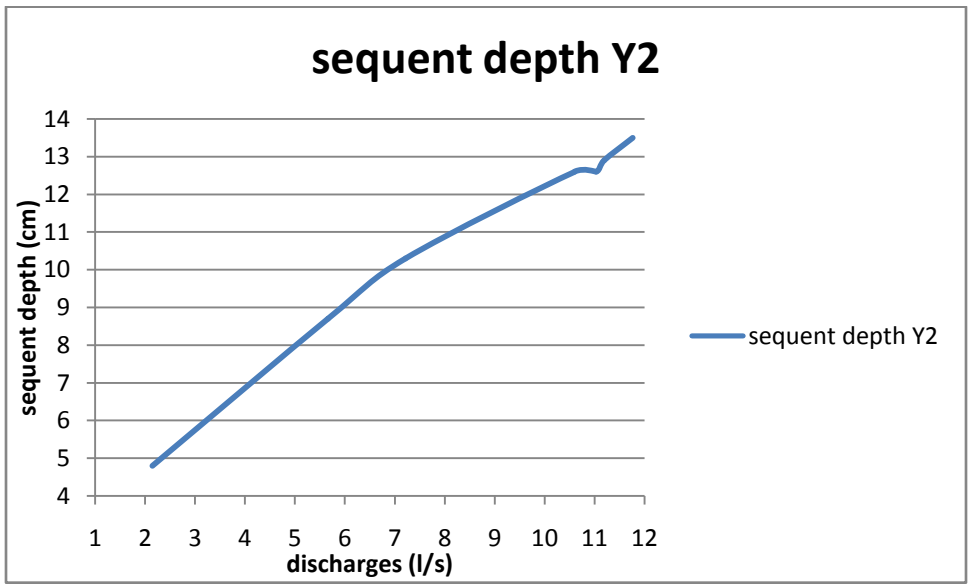


Figure 4.3: Variation of sequent depth with discharge

From figure 4.2, figure 4.3 and table 4.1 above the following was deduced;

1) The flow downstream before the jump was found to be supercritical for all discharges measured as indicated by the Froude number f_1.
2) Jumps were created for all discharges used.
3) The jumps created showed an average dissipation of energy efficiency of 62 percent.
4) The use of this weir would reduce cost of design when used for spillways as it will reduce measures to counteract scouring effect downstream.

5) The sequent depth increases almost linearly with the discharge.

The cost of design of semi-circular weirs has always been high owing to the difficulty encountered in the form-work for the semi-circular crest. However, with recent innovations of design practices, the form-work is now made easily thereby nullifying the effect of difficulty in constructions.

4.3 Measured flow parameter on the semi-circular broad crested weir

The values in tables 4.2(a-d), 4.3(a-d) and 4.4(a-d) were analyzed using regression analysis model to develop equations (4.1) for head-discharge relationship and (4.2) and (4.3) for the discharge coefficients respectively.

Tables 4.2a: Measured and calculated flow parameters for weir models (A1) with R= 5cm and . $\alpha = 90^o$.

	Times (s)												
MASS (Kg)	t_1(s)	t_2(s)	t_3(s)	t_{av}(s)	Q_{act}	height (cm)	H(cm)	V_a(m/s)	H_a(m)	H_{ef}(cm)	h/p	Q_{th}(l/s)	C_d
30	4.51	4.47	4.43	4.47	6.71	24.54	4.54	0.091	0.0004	4.582	0.229	8.683	0.773
30	3.78	3.78	3.79	3.78	7.93	25.00	5.00	0.106	0.0006	5.057	0.253	10.064	0.788
30	3.40	3.44	3.48	3.44	8.72	25.30	5.30	0.115	0.0007	5.367	0.268	11.002	0.793
z30	3.03	3.04	3.00	3.02	9.92	25.77	5.77	0.128	0.0008	5.854	0.293	12.527	0.792
30	2.90	2.92	2.93	2.92	10.29	25.90	5.90	0.132	0.0009	5.989	0.299	12.963	0.793
30	2.73	2.75	2.74	2.74	10.95	26.10	6.10	0.140	0.0010	6.200	0.310	13.649	0.802

Tables 4.2b**:** Measured and calculated flow parameters for weir models (A2) with R= 5cm and $\alpha = 60^o$

	Times (s)												
mass (Kg)	t_1(s)	t_2(s)	t_3(s)	t_{av}(s)	Q_{act}(l/s)	height (cm)	H(cm)	V_a(m/s)	H_a(m)	H_{ef}(cm)	h/p	Q_{th}(l/s)	C_d
30	4.1	4.12	4.07	4.10	7.32	24.34	4.34	0.100	0.0005	4.391	0.220	9.393	0.780
30	3.7	3.65	3.74	3.70	8.12	24.6	4.6	0.110	0.0006	4.662	0.233	10.271	0.790
30	3.27	3.29	3.28	3.28	9.15	24.96	4.96	0.122	0.0008	5.036	0.252	11.529	0.793
30	2.92	3.03	2.95	2.97	10.11	25.28	5.28	0.133	0.0009	5.371	0.269	12.692	0.797
30	2.78	2.82	2.8	2.80	10.71	25.48	5.48	0.140	0.0010	5.580	0.279	13.439	0.797
30	2.65	2.64	2.64	2.64	11.35	25.65	5.65	0.147	0.0011	5.761	0.288	14.094	0.805

Tables 4.2c: Measured and calculated flow parameters for weir models (A3) with R= 5cm and $\alpha = 30^{o}$.

mass (Kg)	Times (s) t_1(s)	t_2(s)	t_3(s)	t_{av}(s)	Q_{act}t(s)	height (cm)	H(cm)	V_a(m/s)	H_a(m)	H_{ef}(cm)	h/p	Q_{th}(l/s)	C_d
30	3.94	3.96	3.98	3.96	7.58	23.05	3.05	0.110	0.0006	3.111	0.156	9.697	0.781
30	3.53	3.54	3.56	3.54	8.47	23.2	3.2	0.122	0.0008	3.275	0.164	10.468	0.809
30	3.15	3.13	3.17	3.15	9.52	23.45	3.45	0.135	0.0009	3.543	0.177	11.769	0.809
30	2.94	2.92	2.92	2.93	10.25	23.61	3.61	0.145	0.0011	3.717	0.186	12.635	0.811
30	2.75	2.83	2.74	2.77	10.82	23.7	3.7	0.152	0.0012	3.818	0.191	13.148	0.823
30	2.63	2.55	2.64	2.61	11.51	23.78	3.78	0.161	0.0013	3.913	0.196	13.629	0.844

Tables 4.2d**:** Measured and calculated flow parameters for weir models (A4) with R= 5cm and $\alpha = 15^{o}$.

Mass (Kg)	Times (s) t_1(s)	t_2(s)	t_3(s)	t_{av}(s)	Q_{act}(l/s)	height (cm)	H(cm)	V_a(m/s)	H_a(m)	H_{ef}(cm)	h/p	Q_{th}(l/s)	C_d
30	3.53	3.56	3.51	3.53	8.49	21.98	1.98	0.129	0.0008	2.065	0.103	10.070	0.843
30	3.19	3.25	3.24	3.23	9.30	22.1	2.1	0.140	0.0010	2.200	0.110	11.063	0.840
30	3.02	3.04	3.03	3.03	9.90	22.18	2.18	0.149	0.0011	2.293	0.115	11.754	0.842
30	2.86	2.85	2.82	2.84	10.55	22.24	2.24	0.158	0.0013	2.367	0.118	12.313	0.857
30	2.67	2.65	2.66	2.66	11.28	22.3	2.3	0.169	0.0014	2.445	0.122	12.897	0.875
30	2.56	2.54	2.55	2.55	11.76	22.34	2.34	0.176	0.0016	2.497	0.125	13.294	0.885

Tables 4.3a: Measured and calculated flow parameters for weir models (A5) with R= 7.5cm and $\alpha = 90^{o}$.

MASS (Kg)	Times (s) t_1(s)	t_2(s)	t_3(s)	t_{av}(s)	Q_{act}(l/s)	height (cm)	H(cm)	V_a(m/s)	H_a(m)	H_{ef}(cm)	h/p	Q_{th}(l/s)	C_d
30	4.61	4.72	4.73	4.69	6.40	24.41	4.41	0.087	0.0004	4.449	0.222	8.307	0.771
30	4.01	4	4.02	4.01	7.48	24.82	4.82	0.100	0.0005	4.871	0.244	9.516	0.786
30	3.53	3.5	3.54	3.52	8.51	25.24	5.24	0.112	0.0006	5.304	0.265	10.810	0.788
30	3.11	3.04	3.12	3.09	9.71	25.69	5.69	0.126	0.0008	5.771	0.289	12.262	0.792
30	2.94	2.95	2.95	2.95	10.18	25.86	5.86	0.131	0.0009	5.948	0.297	12.829	0.794
30	2.77	2.75	2.78	2.77	10.84	26.1	6.1	0.138	0.0010	6.198	0.310	13.643	0.795

Tables 4.3b: Measured and calculated flow parameters for weir models (A6) with R= 7.5cm and $\alpha = 60^o$.

mass (Kg)	Times (s) t_1(s)	t_2(s)	t_3(s)	t_{av}(s)	Q_{act}(l/s)	height (cm)	H(cm)	V_a(m/s)	H_a(m)	H_{ef}(cm)	h/p	Q_{th}(l/s)	C_d
30	4.36	4.33	4.35	4.35	6.90	24.2	4.2	0.095	0.0005	4.246	0.212	8.932	0.773
30	3.84	3.84	3.85	3.80	7.90	24.53	4.53	0.107	0.0006	4.589	0.229	10.031	0.788
30	3.3	3.33	3.28	3.33	9.01	24.92	4.92	0.121	0.0007	4.994	0.250	11.385	0.791
30	3.07	3.05	3.09	3.07	9.77	25.17	5.17	0.129	0.0009	5.255	0.263	12.287	0.795
30	2.95	2.87	2.96	2.93	10.25	25.33	5.33	0.135	0.0009	5.423	0.271	12.877	0.796
30	2.8	2.78	2.8	2.79	10.74	25.46	5.46	0.141	0.0010	5.561	0.278	13.369	0.803

Tables 4.3c**:** Measured and calculated flow parameters for weir models (A7) with R= 7.5cm and $\alpha = 30^o$.

mass (Kg)	Times (s) t_1(s)	t_2(s)	t_3(s)	t_{av}(s)	Q_{act}(l/s)	height (cm)	H(cm)	V_a(m/s)	H_a(m)	H_{ef}(cm)	h/p	Q_{th}(l/s)	C_d
30	4.04	4.04	4.05	4.04	7.42	23.01	3.01	0.107	0.0006	3.069	0.153	9.501	0.781
30	3.25	3.3	3.44	3.33	9.01	23.36	3.36	0.129	0.0008	3.444	0.172	11.283	0.798
30	3.12	3.14	3.13	3.13	9.58	23.5	3.5	0.136	0.0009	3.594	0.180	12.023	0.797
30	3.03	3.01	3.05	3.03	9.90	23.57	3.57	0.140	0.0010	3.670	0.183	12.402	0.798
30	2.8	2.95	2.85	2.87	10.47	23.69	3.69	0.147	0.0011	3.801	0.190	13.064	0.801
30	2.73	2.75	2.77	2.75	10.91	23.77	3.77	0.153	0.0012	3.889	0.194	13.519	0.807

Tables 4.3d: Measured and calculated flow parameters for weir models (A8) with R= 7.5cm and $\alpha = 15^o$.

Mass (Kg)	Times (s) t_1(s)	t_2(s)	t_3(s)	t_{av}(s)	Q_{act}(l/s)	height (cm)	H(cm)	V_a(m/s)	H_a(m)	H_{ef}(cm)	h/p	Q_{th}(l/s)	C_d
30	3.83	3.93	3.93	3.90	7.70	21.95	1.95	0.117	0.0007	2.020	0.101	9.762	0.789
30	3.42	3.41	3.42	3.42	8.78	22.1	2.1	0.132	0.0009	2.189	0.109	10.998	0.798
30	3.05	3.04	3.04	3.04	9.86	22.26	2.26	0.148	0.0011	2.371	0.119	12.371	0.797
30	2.96	2.94	2.95	2.95	10.17	22.3	2.3	0.152	0.0012	2.418	0.121	12.730	0.799
30	2.85	2.88	2.83	2.85	10.51	22.34	2.34	0.157	0.0013	2.465	0.123	13.099	0.803
30	2.55	2.65	2.57	2.59	11.58	22.42	2.42	0.172	0.0015	2.571	0.129	13.911	0.833

Tables 4.4a: Measured and calculated flow parameters for weir models (A9) with R= 10cm and $\alpha = 90^o$

Mass (kg)	Times (s) t_1(s)	t_2(s)	t_3(s)	t_{av}(s)	Q_{act}(l/s)	height (cm)	H(cm)	V_a(m/s)	H_a(m)	H_{ef}(cm)	h/p	Q_{th}(l/s)	C_d
30	4.81	4.74	4.84	4.80	6.25	24.35	4.35	0.086	0.0004	4.387	0.219	8.136	0.769
30	4.12	4.14	4.13	4.13	7.26	24.76	4.76	0.098	0.0005	4.809	0.240	9.333	0.778
30	3.65	3.64	3.54	3.61	8.31	25.17	5.17	0.110	0.0006	5.232	0.262	10.589	0.785
30	3.2	3.18	3.24	3.21	9.36	25.56	5.56	0.122	0.0008	5.636	0.282	11.836	0.790
30	3.08	3.07	3.09	3.08	9.74	25.7	5.7	0.126	0.0008	5.781	0.289	12.296	0.792
30	2.85	2.84	2.89	2.86	10.49	25.98	5.98	0.135	0.0009	6.072	0.304	13.233	0.793

Tables 4.4b**:** Measured and calculated flow parameters for weir models (A10) with R= 10cm and $\alpha = 60^o$

Mass (Kg)	Times (s) t_1(s)	t_2(s)	t_3(s)	t_{av}(s)	Q_{act}(l/s)	height (cm)	H(cm)	V_a(m/s)	H_a(m)	H_{ef}(cm)	h/p	Q_{th}(l/s)	C_d
30	4.47	4.49	4.5	4.49	6.69	24.12	4.12	0.092	0.0004	4.164	0.208	8.673	0.771
30	3.83	3.82	3.83	3.83	7.84	24.54	4.54	0.106	0.0006	4.598	0.230	10.062	0.779
30	3.25	3.23	3.25	3.24	9.25	25.04	5.04	0.123	0.0008	5.117	0.256	11.809	0.783
30	3.16	3.14	3.15	3.15	9.52	25.11	5.11	0.126	0.0008	5.191	0.260	12.065	0.789
30	2.96	3.02	3.04	3.01	9.98	25.26	5.26	0.132	0.0009	5.348	0.267	12.614	0.791
30	2.85	2.85	2.95	2.88	10.40	25.44	5.44	0.136	0.0009	5.535	0.277	13.278	0.784

Tables 4.4c: Measured and calculated flow parameters for weir models (A11) with R= 10cm and $\alpha = 30^o$

Mass (Kg)	Times(s) t_1(s)	t_2(s)	t_3(s)	t_{av}(s)	Q_{act}(l/s)	height (cm)	H(cm)	V_a(m/s)	H_a(m)	H_{ef}(cm)	h/p	Q_{th}(l/s)	C_d
30	4.32	4.31	4.31	4.31	6.96	22.9	2.9	0.101	0.0005	2.952	0.148	8.967	0.776
30	3.77	3.81	3.71	3.76	7.97	23.15	3.15	0.115	0.0007	3.217	0.161	10.194	0.782
30	3.14	3.13	3.16	3.14	9.54	23.5	3.5	0.135	0.0009	3.593	0.180	12.020	0.794
30	3.04	3.03	3.03	3.03	9.89	23.57	3.57	0.140	0.0010	3.670	0.183	12.401	0.798
30	2.94	2.93	2.95	2.94	10.20	23.64	3.64	0.144	0.0011	3.746	0.187	12.784	0.798
30	2.74	2.75	2.75	2.75	10.92	23.79	3.79	0.153	0.0012	3.909	0.195	13.624	0.802

Tables 4.4d: Measured and calculated flow parameters for weir models (A12) with R= 10cm and $\alpha = 15^o$

Mass (Kg)	Times (s) t_1(s)	t_2(s)	t_3(s)	t_{av}(s)	Q_{act}(l/s)	height (cm)	H(cm)	V_a(m/s)	H_a(m)	H_{ef}(cm)	h/p	Q_{th}(l/s)	C_d
30	4.03	4.01	4.02	4.02	7.46	21.93	1.93	0.113	0.0007	1.996	0.100	9.592	0.778
30	3.53	3.54	3.56	3.54	8.47	22.07	2.07	0.128	0.0008	2.153	0.108	10.734	0.789
30	3.27	3.24	3.25	3.25	9.22	22.17	2.17	0.139	0.0010	2.268	0.113	11.586	0.796
30	3.05	3.04	3.03	3.04	9.87	22.26	2.26	0.148	0.0011	2.371	0.119	12.372	0.798
30	2.84	2.84	2.85	2.84	10.55	22.35	2.35	0.157	0.0013	2.476	0.124	13.184	0.800
30	2.62	2.64	2.65	2.64	11.38	22.45	2.45	0.169	0.0015	2.595	0.130	14.123	0.806

The following expressions were developed using the experimental results in tables 4.4(a-d), 4.4(a-d) and 4.5(a-d)

$$Q = \frac{CH^n}{sin\alpha^m} \tag{4.1}$$

Equation (4.1) is the discharge-head relationship which can be adopted in calculating flow rate over any of the semi-circular crested weir models

$$C_d = K \left(\frac{h}{P}\right)^{\beta_1} \left(\frac{R}{P}\right)^{\beta_2} (\sin \alpha)^{\beta_3} \tag{4.2}$$

Equation 4.2 shows the non-linear variation of C_d with$\left(\frac{h}{P}\right)$, $\left(\frac{R}{P}\right)$ and sinα which can be used to determine the coefficient of discharge of each model.

$$C_d = b_o + b_1\left(\frac{h}{P}\right) + b_2\left(\frac{R}{P}\right) + b_3(\sin \alpha) \tag{4.3}$$

Equations (4.3) show the linear variation of C_d with$\left(\frac{h}{P}\right)$, $\left(\frac{R}{P}\right)$ and sinα which can also be used to determine the coefficient of discharge of each model. However, it has a lower regression coefficient.

The parameters were determined using regression analysis as follows:

Table 4.5 Values of parameters as a result of regression analysis

equation	Parameter	value	R^2	Error
4.1	C	0.58	0.986	0.00836
	n	1.611		
	m	1.092		
4.2	K	0.87	0.664	0.007
	β_1	0.109		
	β_2	-0.042		
	β_3	-0.096		
4.3	b_o	0.841	0.574	0.015
	b_1	0.294		
	b_2	-0.095		
	b_3	-0.102		

Tables 4.2(a-d) to 4.4 (a-d) shows the variation of C_d with $\left(\frac{h}{P}\right)$ for crest radius R = 5cm, 7.5cm and 10cm and inclined angles α = 15^o, 30^o, 60^o and 90^o respectively. Hence the following was observed:

1) The coefficient of discharge C_d increases with increase in $\left(\frac{h}{P}\right)$ values and for small values of $\left(\frac{h}{P}\right)$, R = 5cm weir give high values of C_d (figure 4.4). Thus in agreement with Muhammad (2012). This behavior is attributed to the fact that at lower values of $\frac{h}{P}$, the discharge is low and the velocity head of flow can be ignored. While for both R = 7.5 and R =10cm the weir gives an almost linear relationship between C_d and $\frac{h}{P}$.

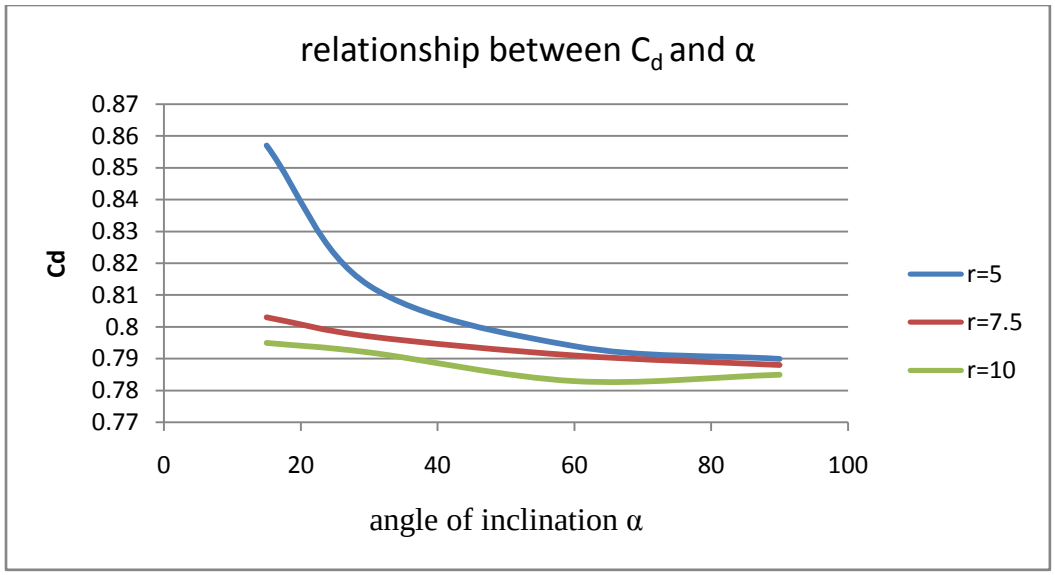


Fig 4.4: Variation of C_d with angle of inclination

2) Weirs of smaller inclination (15^o) give higher values of C_d than those of higher inclination (90^o). This is because weir of small inclination has longer length for discharge.

3) Weirs of smaller crest radius give C_d values higher than those of larger crest radii. This is because weirs with larger radii provide more surface area for flow, hence, effect of friction between the fluid and weir surface becomes more pronounced. It is however, important to note that these points (points 2 and 3) are in agreement with Muhammad (2012) and Noori and Chilmeran (2005).

4) More so, the discharge coefficients 'C_d' obtained by Muhammad (2012) are relatively higher than those obtained in this work. This is because of the larger radii considered in this work.

4.4 Hydraulic Performance of the Semi-Circular Weir Models

In table 4.7 $\left(\frac{h}{P}\right)$ values increases along each column. One may observe that flow magnification factor $\left(\frac{Q_{NC}}{Q_{NS}}\right)$ increases with an increase in value of head to crest height $\left(\frac{h}{P}\right)$ and magnification factor values are always higher than one for all values of $\left(\frac{h}{P}\right)$. That is, for all value of weir height and crest radii, semicircular crested weirs perform better than those of sharp crested. It also agrees with Noori and Chilmeran (2005) as well as Muhammad (2012).

Table 4.6 Performance in terms flow magnification for the semi-circular crested weir models

Magnification factor (Q_{Nc}/Q_{NS}) R=5cm				Magnification factor (Q_{Nc}/Q_{NS}) R=7.5cm				Magnification factor (Q_{Nc}/Q_{NS}) R=10cm			
90^o	60^o	30^o	15^o	90^o	60^o	30^o	15^o	90^o	60^o	30^o	15^o
1.1963	1.2060	1.1972	1.2583	1.1924	1.1950	1.1962	1.1774	1.1895	1.1920	1.1868	1.1610
1.2197	1.2226	1.2407	1.2581	1.2171	1.2187	1.2261	1.1961	1.2048	1.2056	1.1994	1.1812
1.2268	1.2275	1.2431	1.2625	1.2191	1.2243	1.2250	1.1972	1.2148	1.2119	1.2202	1.1941
1.2248	1.2322	1.2468	1.2847	1.2245	1.2302	1.2271	1.2008	1.2228	1.2212	1.2258	1.1984
1.2266	1.2326	1.2645	1.3109	1.2269	1.2311	1.2316	1.1999	1.2252	1.2235	1.2271	1.2035
1.2393	1.2444	1.2974	1.3262	1.2279	1.2420	1.2408	1.2511	1.2251	1.2117	1.2328	1.2123

From table 4.6, the following was observed:

Higher values of magnification factor (better performance) were obtained for weirs of oblique angle, $\propto = 15^o$ than those of 30^o and 60^o due to the fact that weirs of small oblique angles give longer lengths for discharge. Higher values of magnification factor (better performance) were also obtained for weirs of crest radius (R) = 5cm than those of larger crest radius. This is because it has the least surface area for water to flow over.

Finally, $\left(\frac{Q_{NC}}{Q_{NS}}\right)$ increases with the increase in $\left(\frac{h}{P}\right)$. The above points are all in agreement with the findings of Muhammad (2012), Tingey (2011) and Noori and Chilmeran (2005).

However, comparison was made between radius 4.5cm of the compound crested weir studied by Muhammad (2012) and R = 5cm of the semicircular weir, since that was the closest in size obtainable from both works. The compound crested weir has an average performance of 0.8, 0.99 and 1.22 at angles 90^o, 60^o and 30^o respectively. While the semicircular crested weir has an average performance of 1.2, 1.23 and 1.25 at angles of 90^o, 60^o and 30^o respectively. From these it can be said that even though both weirs measure considerable the same in performance at small angles of inclination, the semi-circular weir performed better at higher angle of inclination.

4.5 Developed Model Equations

The parameters of Equations (4.1) and (4.2) have been obtained by regression analysis as indicated in Table 4.6. Equation 4.1 has correlation coefficient of 0.986 that is, 98.6 percent of the variance in the observed values of the dependent variable is explained by the model and 1.4 percent of this variable remains unexplained in the error (residual) term. This applies also to Equation (4.2). Equations (4.1), (4.2) and (4.3) are reliable in predicting discharge and discharge coefficients (table 4.10 and 4.11). This is due to their high correlation coefficients (R^2) and their respective small errors of standard estimate (0.0083, 0.007 and 0.015). However, the equations of discharge coefficients proposed by Noori and Chilmeran (2005) and Muhammad (2012) are better than the developed Equation (4.2) because of their higher correlation coefficient of 0.85 and 0.926 respectively.

Table 4.7: Actual Discharge and Discharges Calculated From Weir Equation Developed

s/n	Q_{act}	H_{ef}(cm)	sinα	Q_{found}
1	6.71	4.582	1	6.736
2	7.93	5.057	1	7.896
3	8.72	5.367	1	8.690
4	9.92	5.854	1	9.995
5	10.29	5.989	1	10.369
6	10.95	6.2	1	10.964
7	7.32	4.391	1.155	7.361
8	8.12	4.662	1.155	8.107
9	9.15	5.036	1.155	9.180
10	10.11	5.371	1.155	10.183
11	10.71	5.58	1.155	10.829
12	11.35	5.761	1.155	11.401
13	7.58	3.111	2	7.695
14	8.47	3.275	2	8.359
15	9.52	3.543	2	9.488
16	10.25	3.717	2	10.250
17	10.82	3.818	2	10.703
18	11.51	3.913	2	11.135
19	8.49	2.065	3.864	8.162
20	9.3	2.2	3.864	9.039
21	9.9	2.293	3.864	9.662
22	10.55	2.367	3.864	10.170
23	11.28	2.445	3.864	10.715
24	11.76	2.497	3.864	11.084
25	6.4	4.449	1	6.424
26	7.48	4.871	1	7.433
27	8.51	5.304	1	8.526
28	9.71	5.771	1	9.768
29	10.18	5.948	1	10.255
30	10.84	6.198	1	10.958
31	6.9	4.246	1.155	6.973
32	7.9	4.589	1.155	7.903
33	9.01	4.994	1.155	9.057
34	9.77	5.255	1.155	9.831
35	10.25	5.423	1.155	10.343
36	10.74	5.561	1.155	10.770

s/n	Q_{act}	H_{ef}(cm)	sinα	Q_{found}
37	7.42	3.069	2	7.528
38	9.01	3.444	2	9.065
39	9.58	3.594	2	9.709
40	9.9	3.67	2	10.042
41	10.47	3.801	2	10.626
42	10.91	3.889	2	11.025
43	7.7	2.02	3.864	7.878
44	8.78	2.189	3.864	8.966
45	9.86	2.371	3.864	10.197
46	10.17	2.418	3.864	10.525
47	10.51	2.465	3.864	10.856
48	11.58	2.571	3.864	11.618
49	6.25	4.387	1	6.280
50	7.26	4.809	1	7.281
51	8.31	5.232	1	8.341
52	9.36	5.636	1	9.402
53	9.74	5.781	1	9.795
54	10.49	6.072	1	10.602
55	6.69	4.164	1.155	6.758
56	7.84	4.598	1.155	7.928
57	9.25	5.117	1.155	9.419
58	9.52	5.191	1.155	9.639
59	9.98	5.348	1.155	10.113
60	10.4	5.535	1.155	10.689
61	6.96	2.952	2	7.071
62	7.97	3.217	2	8.122
63	9.54	3.593	2	9.705
64	9.89	3.67	2	10.042
65	10.2	3.746	2	10.379
66	10.92	3.909	2	11.117
67	7.46	1.996	3.864	7.727
68	8.47	2.153	3.864	8.730
69	9.22	2.268	3.864	9.493
70	9.87	2.371	3.864	10.197
71	10.55	2.476	3.864	10.935
72	11.38	2.595	3.864	11.794

Table 4.8: Actual C_d and C_ds Calculated From Weir Equations of C_d

s/n	Q_{act}	r(cm)	H_{eff}	C_d	h/p	r/p	Sinα	C_d non-linear	C_d linear
1	6.711	5.000	4.582	0.773	0.229	0.250	1.000	0.785	0.783
2	7.930	5.000	5.057	0.788	0.253	0.250	1.000	0.749	0.790
3	8.721	5.000	5.367	0.793	0.268	0.250	1.000	0.752	0.794
4	9.923	5.000	5.854	0.792	0.293	0.250	1.000	0.756	0.801
5	10.286	5.000	5.989	0.793	0.299	0.250	1.000	0.757	0.803
6	10.949	5.000	6.200	0.802	0.310	0.250	1.000	0.759	0.806
7	7.323	5.000	4.391	0.780	0.220	0.250	0.866	0.752	0.793
8	8.115	5.000	4.662	0.790	0.233	0.250	0.866	0.755	0.797
9	9.146	5.000	5.036	0.793	0.252	0.250	0.866	0.759	0.803
10	10.112	5.000	5.371	0.797	0.269	0.250	0.866	0.762	0.808
11	10.714	5.000	5.580	0.797	0.279	0.250	0.866	0.764	0.811
12	11.349	5.000	5.761	0.805	0.288	0.250	0.866	0.766	0.814
13	7.576	5.000	3.111	0.781	0.156	0.250	0.500	0.775	0.812
14	8.467	5.000	3.275	0.809	0.164	0.250	0.500	0.778	0.814
15	9.524	5.000	3.543	0.809	0.177	0.250	0.500	0.782	0.818
16	10.251	5.000	3.717	0.811	0.186	0.250	0.500	0.784	0.821
17	10.817	5.000	3.818	0.823	0.191	0.250	0.500	0.786	0.822
18	11.509	5.000	3.913	0.844	0.196	0.250	0.500	0.787	0.824
19	8.491	5.000	2.065	0.843	0.103	0.250	0.259	0.804	0.821
20	9.298	5.000	2.200	0.840	0.110	0.250	0.259	0.807	0.823
21	9.901	5.000	2.293	0.842	0.115	0.250	0.259	0.809	0.825
22	10.551	5.000	2.367	0.857	0.118	0.250	0.259	0.811	0.826
23	11.278	5.000	2.445	0.875	0.122	0.250	0.259	0.813	0.827
24	11.765	5.000	2.497	0.885	0.125	0.250	0.259	0.814	0.828
25	6.401	7.500	4.449	0.771	0.222	0.375	1.000	0.755	0.769
26	7.481	7.500	4.871	0.786	0.244	0.375	1.000	0.760	0.775
27	8.515	7.500	5.304	0.788	0.265	0.375	1.000	0.764	0.781
28	9.709	7.500	5.771	0.792	0.289	0.375	1.000	0.768	0.788
29	10.181	7.500	5.948	0.794	0.297	0.375	1.000	0.770	0.791
30	10.843	7.500	6.198	0.795	0.310	0.375	1.000	0.772	0.794
31	6.902	7.500	4.246	0.773	0.212	0.375	0.866	0.763	0.779
32	7.902	7.500	4.589	0.788	0.229	0.375	0.866	0.767	0.784
33	9.009	7.500	4.994	0.791	0.250	0.375	0.866	0.771	0.790
34	9.772	7.500	5.255	0.795	0.263	0.375	0.866	0.774	0.794
35	10.251	7.500	5.423	0.796	0.271	0.375	0.866	0.776	0.797
36	10.740	7.500	5.561	0.803	0.278	0.375	0.866	0.777	0.799

Table 4.8: Continued

s/n	Q_{act}	r(cm)	H_{eff}	C_d	h/p	r/p	Sinα	C_d dev non linear	C_d dev. linear
37	7.420	7.500	3.069	0.781	0.153	0.375	0.500	0.788	0.799
38	9.009	7.500	3.444	0.798	0.172	0.375	0.500	0.794	0.805
39	9.585	7.500	3.594	0.797	0.180	0.375	0.500	0.796	0.807
40	9.901	7.500	3.670	0.798	0.183	0.375	0.500	0.797	0.808
41	10.465	7.500	3.801	0.801	0.190	0.375	0.500	0.799	0.810
42	10.909	7.500	3.889	0.807	0.194	0.375	0.500	0.800	0.812
43	7.699	7.500	2.020	0.789	0.101	0.375	0.259	0.816	0.809
44	8.780	7.500	2.189	0.798	0.109	0.375	0.259	0.821	0.811
45	9.858	7.500	2.371	0.797	0.119	0.375	0.259	0.825	0.814
46	10.169	7.500	2.418	0.799	0.121	0.375	0.259	0.826	0.814
47	10.514	7.500	2.475	0.798	0.124	0.375	0.259	0.827	0.815
48	11.583	7.500	2.571	0.833	0.129	0.375	0.259	0.830	0.817
49	6.254	10.000	4.387	0.769	0.219	0.500	1.000	0.763	0.756
50	7.264	10.000	4.809	0.778	0.240	0.500	1.000	0.768	0.762
51	8.310	10.000	5.232	0.785	0.262	0.500	1.000	0.772	0.768
52	9.356	10.000	5.636	0.790	0.282	0.500	1.000	0.776	0.774
53	9.740	10.000	5.781	0.792	0.289	0.500	1.000	0.778	0.776
54	10.490	10.000	6.072	0.793	0.304	0.500	1.000	0.780	0.781
55	6.686	10.000	4.164	0.771	0.208	0.500	0.866	0.771	0.766
56	7.840	10.000	4.598	0.779	0.230	0.500	0.866	0.777	0.773
57	9.250	10.000	5.117	0.783	0.256	0.500	0.866	0.782	0.780
58	9.524	10.000	5.191	0.789	0.260	0.500	0.866	0.783	0.781
59	9.978	10.000	5.348	0.791	0.267	0.500	0.866	0.784	0.784
60	10.405	10.000	5.535	0.784	0.277	0.500	0.866	0.786	0.787
61	6.955	10.000	2.952	0.776	0.148	0.500	0.500	0.795	0.786
62	7.972	10.000	3.217	0.782	0.161	0.500	0.500	0.800	0.790
63	9.544	10.000	3.593	0.794	0.180	0.500	0.500	0.806	0.795
64	9.890	10.000	3.670	0.798	0.183	0.500	0.500	0.807	0.796
65	10.204	10.000	3.746	0.798	0.187	0.500	0.500	0.808	0.798
66	10.922	10.000	3.909	0.802	0.195	0.500	0.500	0.810	0.800
67	7.463	10.000	1.996	0.778	0.100	0.500	0.259	0.826	0.796
68	8.467	10.000	2.153	0.789	0.108	0.500	0.259	0.830	0.799
69	9.221	10.000	2.268	0.796	0.113	0.500	0.259	0.833	0.800
70	9.868	10.000	2.371	0.798	0.119	0.500	0.259	0.835	0.802
71	10.551	10.000	2.476	0.800	0.124	0.500	0.259	0.838	0.803
72	11.378	10.000	2.595	0.806	0.130	0.500	0.259	0.840	0.805

4.6 Cost Implication Analysis

The cost implication of the prototypes of the models in the scale of 1:4 is considered. The prototype was made of concrete. The cost analysis is shown below.

The cost of the wet concrete is taken as ₦ 45,000.00 per cubic meter (m^3), as obtained at ELCENA Engineering Limited, 27 Maaji Road, Sabo Tasha, Kaduna.

Table 4.9a Cost Analysis of Semi-Circular Weir

S/N	Description	Unit	Rate (Naira/m^3)	Amount (Naira/m)
1	Volume of concrete for semi-circular crested weir Volume = area × length Area of weir = $3028.3cm^2$ Volume = 3028.3×100 $= 0.302830\times10^6\ cm^3$ $=0.30283m^2$	m^3	45,000	13,700

Table 4.9b Cost Analysis of Sharp Crested Weir

S/N	Description	Unit	Rate (Naira/m^3)	Amount (Naira)
2	Volume of concrete for sharp crested weir Volume = area × length Area of weir = $2919.2cm^2$ Volume = $2919.2\times100cm$ $= 0.29192\times10^6\ cm^2$ $=0.2919m^2$	m^3	45,000	13,200

Weir performance between the oblique semi-circular crested weir and sharp crested oblique weir is about 1.5461. Comparing the costs of construction of models (using a prototype of scale of 1:4), the difference of about ₦1000.00, was obtained. The importance of weir performance at the present is quite obvious. Hence ₦1000.00 is not too expensive to obtain an increase of 54.61 percent weir performance as considered in this study.

CHAPTER FIVE

CONCLUSIONS AND RECOMENDATIONS

5.1 CONCLUSIONS

Within the limits of experimental study for the hydraulic flow characteristics over semi-circular crested weir models, the following conclusions were drawn which are in agreement with the findings for different weir shapes studied by Borghei et al (2003), Noori and Chilmeran (2005), Thair and Tahseen(2006), Kabirri-Samani et al (2010) , Tingey (2011) and Mujahid (2012).

1. For normal weir with $\alpha = 90^o$, the relation between (C_d) and $\left(\frac{h}{P}\right)$ shows that an increase in $\left(\frac{h}{P}\right)$ value leads to increases in (C_d) value for the same weir height.
2. Relations between (C_d) and $\left(\frac{h}{P}\right)$ show that for oblique weirs (C_d) increases with increase in $\left(\frac{h}{P}\right)$ and for small values of $\left(\frac{h}{P}\right)$ the weir gives high values of (C_d).
3. An equation for discharge coefficient (C_d) estimation in terms of $\left(\frac{h}{P}\right)$, $\left(\frac{R}{P}\right)$ and sinα was obtained.
4. Flow magnification factor $\left(\frac{Q_{NC}}{Q_{NS}}\right)$ for normal weirs increases with increase in $\left(\frac{h}{P}\right)$ value and is greater than one for all $\left(\frac{h}{P}\right)$ values.
5. High performance in term of $\left(\frac{Q_{NC}}{Q_{NS}}\right)$ was achieved with weirs of small oblique angles. $\left(\frac{Q_{NC}}{Q_{NS}}\right)$ for oblique weirs increases with the increase of $\left(\frac{h}{P}\right)$ values.
6. The weir model with angle of inclination of $\propto = 15^o$ with the crest radius of R = 5cm perform best among the rest of the models.

This study has therefore been able to achieve the following:

1. Develop a calibrated weir model equation that can be used to estimate discharge over the weir models for all angle of inclination tested.
2. Developed a mathematical model for predicting coefficients of discharge 'C_d' for these models which can be used for the design of normal and inclined semi-circular crested weir.
3. Placing the weir at an oblique angle is an effective way of increasing discharge in channels without sacrificing freeboard.
4. Also, using a semi-circular crest configuration is an effective way of overcoming the problems of passing more discharge over sharp crested weir without sacrificing freeboard.

5.2 Recommendation

The following recommendations are offered for related research in flow characteristics of weirs and for various applications of weirs in the field of engineering**.**

1. The equation (4.1) proposed can be used for the estimation of the flow rate over semi-circular crested weir depending on the angle of inclination to the direction of flow.
2. Equations (4.2) and (4.3) can be used in predicting the discharge coefficient (C_d) as it has a good correlation coefficient.
3. More research is needed on the nature of the jump and sequent depth when the flow is critical and subcritical for semi-circular broad crested weirs.

REFERENCE

Aichel O.G. (1953) “Discharge Ratios for Oblique Weirs,” Abusszahlen fur schiefe weher, Z.VDI, 95 (1), pp. 26 - 27.

Abid-Ali, H.S (1986) Characteristics of Flow Over the Round crested weir. M. Sc Thesis, University Busra Iraq

Al – Tikrity, R.A.H.,(2000) "Discharge Coefficient for Semi-Circular Crested Rectangular 'Weirs", M.Sc. Thesis, Department of Civil Engineering, University of Tikrit, Iraq, 2000.

Al Babely (2011) “Overflow Characteristic of Cylindrical Shape Crest Weirs Over Horizontal Bed” Tikrit Journal of Engineering Sciences Vol.18/No. 4 December, (92-39)

Al Babely E.A,(2012) “Behavior of the Discharge Coefficient for the Overflow Characteristics of Oblique Circular Weirs” Tikrit Journal of Engineering Sciences/Vol.19/No.4/December, (55-64)

Al-Hasson, H. M.(1978), “Hydraulic of Flow Over Labyrinth Weirs”, Ph. D. Thesis, Department of Civil Engineering, Southampton University, Southampton, England.

Al-Neima, (1983)., "Prediction of Discharge Coefficient for Inclined 'Weirs", M.Sc. Thesis, Dept. of Irrigation and Drainage Engineering, University of Mosul, Iraq.

Al-Tabatabaie, F.A., Al-Nassiri, A.h, {S. and Al-Zubaitle, R.M., "Characteristics of Flow Over TheSerni-Circular Crested Weirs", Journal af Engineering and technology, 3 (4): 157-159.

British Standard Institute (1965). Methods of Measurement of Liquid Flow in Open Channels, Part 4, BS 3680, BSI, London, England.

Bos, M.G (1989). Discharge Measurement Structures, International Institute if Land Reclamation And Improvement, Third Edition, Wageningen, Netherlands.

Borghei, S.M., Kabiri – Samani, A.R., and Nekoee, N., (2006), "Oblique Weir Equation Using Incomplete Self-Similarity," Canadian Journal of Civil Engineering, 33, pp. 1241-1250.

Borghei, S.M., Vatannia Z., Ghodsian, and M., Jalili, M.R,(2003), "Oblique Rectangular Sharp-Crested Weir," Water and Maritime Engineering 156, WM2, pp. 185-191.

Chanson, H. and Montes ,J.S.(1998),"Overflow Characteristics of Circular Weirs", Proc. ASCE, Journal of lrrigation and Drainage Engineering, 124(3), 152-162.

Chilmeran, T.A.H. (1996), "Characteristics of Flow Over Normal and Oblique Weirs with Semi-Circular Crests", M.Sc. Thesis, Dept. of Irrigation and Drainage Engineering, University of Mosul, Iraq.

Chow, V. T. (1959), "Open Channel Hydraulics," second edition, McGraw-Hill Book Company Inc., New York.

Darvas, L. A.(1971) , Discussion on : "Performance and Design of Labyrinth Weirs", Journal of Hydraulic Division of the ASCE, No.HY8, August 1971, PP. 1246-1251.

De Vries, M., (1959), "Oblique Weirs," Report WL, Delft Hydraulics, In Dutch. Department of Civil Engineering, Southampton University, Southampton, England,

Franzini, J.B. and Finnemore, E.J. (1997). "Fluid Mechanics with Engineering Applications." McGraw-Hill Company Inc, New York.

Henderson, F. M., (1966) Open Channel Flow, Macmillan, New York, pp. 174- 176.

Ibraheem, G. M.(1983), "Discharge and Flow Characteristics of Weirs with Triangular Plan Form", M. Sc. Thesis, University of Mosul, Mosul, Iraq.

Kabiri-Samani A.,Ansari, A. and Borghei, S. M (2010). Hydraulic Behaviuor of Flow Over an Oblique Weir. Journal of Hydraulic Research, 5 (48) p 669-673.

Kinsdvater, C. E. and Cater, R. W. (1957). “Discharge Characteristics of Rectangular Thin-Plate Weirs.” Journal of Hydraulics Division, Vol. 83, No. 6, December, 1-36.

Matthew, G.D.(1963); "On the Influence of Curvature, Surface Tension and Viscosity on Flow Over Round-Crested Weirs", Proc. Inst" Civil Ercgineers, 25, 511-524.

Muhammad, M. M (2012); “Experimental study of flow characteristics over compound crested weir” M. sc Thesis, Department of Water Resources and Environmental Engineering, Ahmadu Bello University, Zaria.

Munson, B. R., Young, D. F. and Okiishi, T. H. (2002); “Fundamentals of Fluid Mechanics.” John Wiley & Sons Inc., New York, USA.

Nawzad O"A. (2004); “An Experimental Investigation of the Coefficient of Discharge for Circular and Semi-Circular Weirs” Journal of ZankeySulaimani, April,Vol,7(1)Part A(87-94).

Noori and Jaafar,(2011); ‘Crest Shape Effect on the Performance of Rectangular Side Weirs” Al-Rafidain Engineering Vol.19 No.5 October.

Noori, B.M.A., and Chilmeran, T.A..(2005); “Characteristics of Flow over Normal and Oblique Weirs with Semicircular Crests,” Al_Rafidain Engineering, **13**(1), pp. 49-61.

Ramamurthy ,A.S. (1993),"Characteristics of Circular Crested Weir", Proc.ASCE ,Journal of the Hydraulic Engineering , ,119(9) , 1055-1061.

Rao, N.S.L. and Rao, M.V.J.(I 973);"Characteristics of Hydrofoil Weirs",Proc" ASCE, Journal of the Hydraulic D ev is ion., 99(HY2), 259 -283 "

Rehbock, T. (1929); “Discussion of ‘Precise Measurements’.” By K. B. Turner. Trans., ASCE, Vol. 93, 1143-1162.

Smith, R.A.,(1959)"Calibration of a Submerged Broad Crested Weir" , Proc. ASCE, Journal of the Hydraulics Devision, , 85(HY3), 1-16.

Sisman H.G, (2009), Experimental Investigation of Sharp Crested Rectangular Weirs, M. Sc Thesis, Department of Civil Engineering, Middle East Technical University, Ankara.

Subramanya, K. (1986). "Flow in Open Channels." McGraw-Hill Publishing Company Limited

Thair M. A and Tahsen A. H. C. (2006). Hydraulic Charateristics of Flow Over Compound Crested Weir. Al-Rafidain Journal of Engineering, 2 (14): p 81-87.

Tullis, J.P., Nosratollah, A., and Waldron, D. (1995), "Design of Labyrint Spillways," Journal of Hydraulic Engineering, 121(3), pp. 247-255.

Tuyen, N.B., (2006), "Flow over Oblique Weirs," Unpublished MSc. Thesis, Delft University of Technology, Netherlands.

Uijttewaal, W.S.J., (2007), "Inundated Flood Plains and the Flow over Groynes and Oblique Weirs," Publs. Geophys. Pol. Acad. Sc., E-7 (401), pp. 245-254.

Willmore, C.,(2004), "Hydraulic Characteristics of Labyrinth Weirs," M.S. Report, Utah State University, Logan, UT.

Wols, B., Uijttewaal, W., Labeur, R., and Stelling, G., (2006), "Rapidly Varying Flow over Oblique Weirs," Proceedings of the 7th International Conference onHydro-science and Engineering, Philadelphia, PA, pp. 1-13.

APPENDIX

APPENDIX A



Plate V: weirs of radius 5cm



plate VI: weirs of radius 7.5cm



Plate VII: weirs of radius 10cm



Plate VIII: showing flow over normal weir



Plate IX: showing plan of normal weirs



plate X: showing down stream flow

APPENDIX B**:** Water depth for different discharge conditions

	Q_1	Q_2	Q_3	Q_4	Q_5	Q_6	Q_7
Distance from the weir (cm)	Water depth from the bottom of channel (cm)						
300	20	22	22.7	23.4	23.6	23.8	24.8
290	20	22	22.7	23.4	23.6	23.8	24.8
280	20	22	22.7	23.4	23.6	23.8	24.8
270	20	22	22.7	23.4	23.6	23.8	24.9
260	20.2	22	22.7	23.4	23.6	23.9	24.9
250	20.2	22	22.7	23.4	23.7	23.9	24.9
240	20.2	22	22.7	23.5	23.7	23.9	24.9
230	20.2	22.1	22.8	23.5	23.7	23.9	24.9
220	20.2	22.1	22.8	23.5	23.7	23.9	24.9
210	20.2	22.1	22.8	23.5	23.7	23.9	24.9
200	20.2	22.1	22.8	23.5	23.7	23.9	24.9
190	20.2	22.1	22.8	23.5	23.7	23.9	24.9
180	20.2	22.1	22.8	23.5	23.7	23.9	24.9
170	20.2	22.1	22.8	23.5	23.7	23.9	24.9
160	20.2	22.1	22.8	23.5	23.7	23.9	24.9
150	20.2	22.1	22.8	23.5	23.7	23.9	24.9
140	20.2	22.1	22.8	23.5	23.7	23.9	24.9
130	20.2	22.1	22.8	23.5	23.7	23.9	24.9
120	20.2	22.1	22.8	23.5	23.7	23.9	24.9
110	20.2	22.1	22.8	23.5	23.7	23.9	24.9
100	20.2	22.1	22.8	23.5	23.7	23.9	24.9
90	20.2	22.1	22.8	23.5	23.7	23.9	24.9
80	20.2	22.1	22.8	23.5	23.7	23.9	24.9
70	20.2	22.1	22.8	23.5	23.7	23.9	24.9
60	20.2	22.1	22.8	23.5	23.7	23.9	24.9
50	20.2	22.1	22.8	23.5	23.7	23.9	24.9
40	20.2	22.1	22.8	23.5	23.7	23.9	24.9
30	20.1	22	22.8	23.5	23.6	23.9	24.9
20	20	21.8	22.6	23.3	23.5	23.8	24.8
10	19.8	21.7	22.5	23.2	23.4	23.6	24.7
0	19.7	21.6	22.4	23.1	23.2	23.5	24.5

APPENDIX C**:** Water depth for seven different discharges downstream of the weir (Q_1 to Q_7)

distance from the weir downstream (cm)	height of water from the bottom of the channel for (cm)						
	Q_1	Q_2	Q_3	Q_4	Q_5	Q_6	Q_7
10	1.3	4.75	3.7	2.7	2.9	2.6	2.6
20	1.4	4.8	3.7	2.6	2.9	2.6	2.6
30	1.5	5.2	3.9	2.7	3.3	2.6	2.7
40	1.6	5.7	4.8	2.1	3.6	2.5	2.6
50	2.3	5.9	6.6	2.6	6.4	2.5	2.4
60	2.6	6.4	7.5	2.6	7.8	2.6	2.7
70	3.7	6.5	7.8	2.4	8.3	2.8	5.1
80	4.3	7	8.4	2.8	8.7	3.1	8.1
90	4.6	7.1	9	2.2	9.3	3.6	9.4
100	4.6	7.2	9.2	2.6	10.1	8.4	10.8
110	4.6	7.5	9.6	5	10.5	9.6	11.8
120	4.7	8	9.5	9.1	10.8	10.3	12.1
130	4.7	8	9.8	10.5	11.3	10.9	12.4
140	4.7	8	9.8	10.9	11.7	11.9	12.8
150	4.7	8.1	9.9	11.4	12.4	12.8	13.3
160	4.7	8.1	10.2	11.6	12.6	12.9	13
170	4.6	8.7	10.3	12.1	12.5	13.1	13.5
180	4.8	8.4	10.3	12.3	12.5	12.8	13.2
190	4.8	8.7	10.2	12.6	12.6	13.1	13.6
200	4.8	8.6	10.3	12.5	12.7	12.9	13.2
210	4.7	8.7	10.2	12.7	12.6	13	13.1
220	4.7	8.7	10.3	12.8	12.7	13	13.2
230	4.8	8.6	10.3	12.9	12.8	12.9	13.5
240	4.8	8.7	10.2	12.8	12.7	13	13.5
250	4.7	8.6	10.1	12.8	12.6	13	13.6
260	4.8	8.7	10.3	12.9	12.7	12.8	13.6
270	4.9	8.7	10.3	12.9	12.5	12.9	13.5
280	4.7	8.7	10.3	12.9	12.6	13.1	13.6
290	4.8	8.7	10.2	12.9	12.7	13	13.6
300	4.8	8.7	10.3	13	12.8	13	13.6